CHARACTERIZING THE ROLE OF *MTW1* IN THE KINETOCHORE OF THE PATHOGENIC YEAST *CRYPTOCOCCUS NEOFORMANS*

A Thesis Submitted to the Faculty of
the Graduate School of Western Carolina University
in Partial Fulfillment of the Requirements for the Degree of
Master of Science in Biology

By

James Ryan Simmons

Director: Dr. Indrani Bose
Assistant Professor of Biology
Biology Department

Committee Members:
Dr. Seán O'Connell, Biology
Dr. Sabine Rundle, Biology

July 2013

ACKNOWLEDGEMENTS

I would like to thank my advisor, Dr. Indrani Bose, for her guidance and patience throughout this process. I would also like to thank members of the Bose lab, especially Beth Budden and Kathy Turnbull, for their help in performing lab work. In addition, I would like to thank my thesis committee: Dr. Seán O'Connell, Dr. Sabine Rundle, and thesis reader Dr. Greg Adkison.

TABLE OF CONTENTS

LIST OF TABLES

LIST OF FIGURES

LIST OF TERMS/ABBREVIATIONS

BCS	Bathocuproine disulfonic acid
CDE	Centromere DNA Element
ChIP	Chromatin Immunoprecipitation
DTT	dithiothreitol
gDNA	Genomic DNA
KN99	WT, Serotype A strain
LB	Luria-Bertani
NEB	New England Biolabs
PBS	Phosphate-buffered saline
ts	Temperature-sensitive
SDS	Sodium dodecyl sulfate
WT	Wild type
YPD	Yeast extract, peptone, dextrose

GENE ABBREVIATIONS

CSE4	Chromosome Segregation 4
CTR4	Copper Transporter 4
DAD1	*DUO1* and *DAM1* interacting
DAD2	*DUO1* and *DAM1* interacting
DSN1	Dosage Suppressor of *NNF1*
MIF2	Mitotic Fidelity 2
MIS12	Mini-chromosome Segregation
MTW1	*MIS12*-like protein
NNF1	Necessary for Nuclear Function
NSL1	*NNF1* Synthetic Lethal 1

ABSTRACT

CHARACTERIZING THE ROLE OF *MTW1* IN THE KINETOCHORE OF THE PATHOGENIC YEAST *CRYPTOCOCCUS NEOFORMANS*

James Ryan Simmons, M.S.

Western Carolina University (July, 2013)

Advisor: Dr. Indrani Bose

Cryptococcus neoformans is a basidiomycetous yeast with clinical importance due to its role as an opportunistic pathogen in immunocompromised individuals. Upon exposure to *C. neoformans* patients may develop a disease known as cryptococcosis, a condition associated with pulmonary infections that may result in lethal meningoencephalitis. This disease is often accompanied by aneuploidies of single or multiple chromosomes in a subpopulation of the infecting cells, leading to the idea that missegregation of chromosomes during infection may be a way for this organism to deal with stresses and acquiring antifungal resistance. Because this species is rapidly developing resistance to many of the prevalent antifungal treatments, a need exists for more potent therapies with fewer side effects. The molecular biology concerning cellular reproduction and division in *C. neoformans* is poorly understood for such an important fungal pathogen. The research performed so far has produced information about such structures as the centromeric DNA of their chromosomes and the kinetochore protein superstructure that links the spindle microtubules to the centromeres. Understanding how chromosome segregation occurs in *C. neoformans* may bring about better therapies: if it can be shown that homologous proteins perform the same actions in *Cryptococcus* as

they do in other organisms then these proteins may potentially become targets for future studies to determine the mechanism linking the presence of antifungal chemicals to aneuploidy.

The kinetochore protein complex is essential for segregation of chromosomes. Previous experiments have described a protein essential to the structure and function of the yeast kinetochore. The necessity of this protein for kinetochore function was first determined using an *Schizosaccharomyces pombe* strain carrying a temperature-sensitive mutation in the *Mis12* gene that causes the protein to malfunction above a certain temperature. It was found that when grown above the restrictive temperature cells were unable to complete mitotic segregation, with the dividing nucleus stuck in the neck between budding cells. A later study described the budding yeast homolog *MTW1* (Mis12-like protein) in *Saccharomyces cerevisiae* using a similar temperature-sensitive mutant and yielded similar results. This protein is part of a subcomplex of kinetochore proteins called the MIND complex. One goal of this project is to characterize the *MTW1* homolog in *C. neoformans* in order to determine whether it maintains the functional importance to kinetochore structure exhibited by the previously described homologs. This has been addressed through the construction of similar temperature-sensitive mutants and by regulating the gene expression through regulatable *CTR4* promoter. These strains were created through the use of overlap PCR and biolistic transformation. Molecular and phenotypic characterizations have been performed on these strains and include growth and morphological analyses. Results have confirmed the presence of the desired mutations and have shown some inhibitory effect on growth under restrictive conditions. RNA interference was performed in an effort to demonstrate the necessity of

various kinetochore proteins. Initial results indicate that *MTW1*, along with the outer kinetochore gene *DAD2*, are not essential whereas several other MIND complex genes (*NNF1*, *DSN1*) and inner (*CSE4*, *MIF2*) and outer (*DAD1*) kinetochore genes were shown to be necessary for viability of the yeast cells. These results are in accordance with those obtained through the use of strains with conditional mutations in *MTW1*. These results imply that while *CnMTW1* probably acts in the same capacity as that of its ascomycetous homologs and is necessary for optimal kinetochore function, it is not essential for chromosome segregation.

INTRODUCTION

Cryptococcus neoformans

The fungal kingdom is divided into seven phyla with the two largest groups put together in the subkingdom Dikarya: Basidiomycota, (known for specialized reproductive cells called basidiospores that form at the end of basidia and including mushrooms, puffballs, and some yeasts), and Ascomycota (characterized by the formation of sac like structures known as asci in which spores develop and include truffles and several economically important species of yeast). *Cryptococcus neoformans* is a basidiomycetous fungus of the class Tremellomycetes that can be found in the soil throughout much of the world. *C. neoformans* is an opportunistic human pathogen – infection with *C. neoformans* and the resulting meningitis is responsible for approximately 625,000 deaths each year, mostly affecting people with HIV/AIDS (Park et al., 2009). This species is found in human patients suffering from cryptococcosis as an asexual yeast while the sexual perfect state, or teleomorph, of this organism involves microscopic hyphae as opposed to a visible fruiting body and has not been associated with pathogenesis. Several independent observations during the last decade of the nineteenth century led to the discovery, description, and classification of this fungus. The first definitive description of this species occurred in 1894 when the German physicians Busse and Buschke determined that a patient's symptoms were caused by a fungal infection termed cryptococcosis (Casadevall and Perfect, 1998). In the following year a yeast species was isolated from peach juice and shown to cause the formation of neoplasms in animal tissues. Soon thereafter the same species of fungus was isolated

from lesions in a human patient, confirming that this species had the potential for pathogenicity in humans. Since this time, this fungus has been shown to infect many human tissues, including the central nervous system, skin, and lungs.

Little progress was made in the following decades in terms of treatment of cryptococcal infections or in terms of understanding the fungus's pathogenic mechanisms; however, the classification of this species was refined. This species was first named *Saccharomyces hominis* by Busse after its initial discovery in a human patient and was subsequently classified as several other species in the genus *Saccharomyces* such as *S. neoformans* and *S. tumefaciens*, both of whose names imply the formation of neoplastic lesions. The name *Cryptococcus* was first used to describe the genus in 1901 by Vuilleman due to the fact that this fungus does not form ascospores (despite Buschke's initial assertion, which was later redacted) or ferment sugars as other species of *Saccharomyces* do (Casadevall and Perfect, 1998), whereas the species name most commonly used today, *Cryptococcus neoformans*, was formalized in 1950 (Benham, 1950).

Much work was performed in the 1950's to describe the ecology and virulence of *C. neoformans* and it was during this time that the first effective medical treatments were established. Early in the decade, *C. neoformans* was isolated from soil contaminated with pigeon excrement; this discovery lent support to the concept that the infections (such as cryptococcosis) could be acquired from the environment (Casadevall and Perfect, 1998). For the first time, medicines were now available to combat the infection. The development of the first such drug to be efficacious in humans, a polyene antifungal chemical called Amphotericin B, in 1955, from the bacterium *Streptomyces nodosis* led

to further advances in the treatment and understanding of cryptococcal infection. It was later found that using this chemical in conjunction with 5-fluorocytosine reduced the mortality rate of cryptococcal meningitis by approximately two-thirds (Medoff et al., 1972). Further studies into the pathogenesis of *Cryptococcus* sought to associate the establishment of this infection with a site of infection in the body. The presence of nodules in lung tissue and the new understanding that this infection was acquired from the environment and that *C. neoformans* is capable of aerosolization led to the idea that this microbe enters the human body through pulmonary tissue (Casadevall and Perfect, 1998).

Another line of research sought to describe the antigenic properties of the polysaccharide capsule. It was discovered early on that the capsule was a virulence factor that was responsible for interfering with host defense mechanisms such as leukocyte migration and phagocytosis. By 1968, four serotypes had been described (A, B, C, and D) that differ in the unique chemical composition of the capsule's polysaccharide chains, which together are characterized by long unbranched α-1,3-mannan polymers decorated with gulcuronic acid and xylose monosaccharides (Casadevall and Perfect, 1998). These chemical differences result in different levels of virulence, with serotypes A and D being the more prevalent pathogens for immunocompromised patients in the Western hemisphere while serotypes B and C are mostly restricted to tropical and subtropical locations. Two varieties of *C. neoformans* are now described: var *neoformans* (which constitutes serotype D), and var *grubii* (which constitutes serotype A). Serotypes B and C belong to a variety known as var *gattii*,

which is now considered to be a different species within the same genus known as *Cryptococcus gattii* (Enache-Angoulvant et al., 2007).

Cryptococcus neoformans is also known to be virulent due to its biosynthesis of melanin. *C. neoformans* is unique in the genus in that it is the only species with a phenoloxidase enzyme capable of autooxidatively converting diphenolic compounds to the pigment melanin. The role of melanin in virulence was first demonstrated in the early 1980's by several groups who generated mutants incapable of melanin biosynthesis and were able to show that these strains yielded much higher survival times in animals infected with the mutant strains than those seen in animals exposed to wild type *C. neoformans* (Kwon-Chung et al., 1986). Chemical studies suggested that melanin acts as an antioxidant, protecting the fungal cell from oxidation within its host, whereas other studies have shown that melanin permits the cell to evade phagocytosis and protects the cell from damage by ultraviolet light. It is hypothesized that *C. neoformans* may have evolved the laccase enzyme for its ecological niche in the degradation of phenolic compounds of decaying wood in trees (especially those of the genus *Eucalyptus*). It is further thought that the high concentrations of phenolic compounds in the central nervous system may be why this species localizes to these tissues (Casadevall and Perfect, 1998).

Other virulence factors associated with *C. neoformans* include urease (Cox et al., 2000) and phospholipase (Cox et al., 2001) production and the ability for cells to survive and multiply at 37°C (Kraus et al., 2004). Of the 39 species of the *Cryptococcus* genus, *C. neoformans* is the only one able to survive at 37°C (Casadevall and Perfect, 1998) and the ability to grow at high temperatures is considered to be a virulence factor because it is necessary to survive in mammalian hosts. Several proteins, including Ras1p and

calcineurin, are essential for growth at this temperature. Transcription of genes involved in nucleotide and amino acid biosynthesis decreases at 37°C, whereas genes induced by this condition include trehalose synthase, catalase, and superoxide dismutase. Additionally, expression of two heat shock proteins increased two- to three-fold after three hours at 37°C, presumptively in order to help in protein folding (Kraus et al., 2004). Growth at this temperature has also been reported to induce morphological changes in diploid strains (Sia et al., 2000).

The genome of *Cryptococcus neoformans* contains 19 million base pairs encoding approximately 6572 genes across fourteen chromosomes (Loftus et al., 2005). Unlike *Saccharomyces cerevisiae*, the genome of *C. neoformans* lacks a historical entire genome duplication event. The presence of antisense transcripts and the molecular machinery for RNA interference in the genome implies that RNAi plays a role in the regulation of gene expression (Dumesic et al., 2013). At least thirty genes have been associated with the biosynthesis of the extensive polysaccharide capsule that forms outside of the cell wall and have been associated with pathogenesis, while at least fifty extracellular mannoproteins likely are associated with the cell wall and are a unique feature of *C. neoformans* (Loftus et al., 2005). Five percent of the genome is composed of rDNA repeats, while another five percent consists of transposons that are clustered on each chromosome in 40 to 100 kb blocks that may be sequence-independent regional centromeres like those seen in *Schizosaccharomyces pombe*. A common motif in these blocks is the presence of Tcn5/6 transposons, which are thought to mark centromeres (Loftus et al., 2005).

The Role of Aneuploidy in Drug Resistance

In addition to the medicines developed earlier on, Fluconazole, an azole derivative, was later found to also be effective in preventing the development of cryptococcal meningitis. However, long-term therapy has been associated with the appearance of resistant strains (Sionov et al., 2010). Such phenomena have been described in ascomycetous species and were often found to be the result of increased expression of multidrug transporters and transcription factors that influence genes coding for efflux pumps, perturbations in the ergosterol biosynthetic pathway, and activation of heat shock protein Hsp90p (Sionov et al., 2010). This is thought to happen in a stepwise manner with cells withstanding increasingly higher concentrations of fungicide; however, resistance is lost after approximately 26 passages on non-selective media (Sionov et al., 2010). Microarray analysis of one Fluconazole-resistant strain revealed that upregulation of gene expression was largely localized to genes on chromosomes 1 and 4. Comparative genome hybridization, quantitative real time PCR, and Southern blots all showed that this strain was probably disomic for these two chromosomes (Sionov et al., 2010). This is significant as a clone with disomic chromosomes has never been isolated from a stress-free environment, implying a direct role for aneuploidy in azole resistance. A dose-dependent relationship was also noted as higher concentrations of fungicide resulted in more chromosomes being duplicated. One gene associated with both Fluconazole resistance and the chromosome duplication is *ERG11*, which encodes a demethylase that is the target of Fluconazole. This gene is present on chromosome 1; it was therefore thought that the increased expression resulted in Fluconazole resistance. Another gene associated with resistance is *AFR1*, an ATP Binding Cassette (ABC) transporter-

encoding gene. Deletion of this gene resulted in decreased Fluconazole resistance (along with resistance to other drugs such as cycloheximide and rhizoxin) while overexpression resulted in increased resistance (Sionov et al., 2010). Drug export is particularly important to *C. neoformans*, which has twice as many genes involved in drug transport than *S. cerevisiae*. Fluconazole may have a direct effect on chromosome segregation, either on spindle pole body segregation or through its repressive effect on ergosterol synthesis, which is required for proper cytokinesis due to role of ergosterol in forming new cell walls and membranes.

More insights into the mechanisms behind aneuploidy have arisen from the study of apoptosis-like cell death (ALCD) in *C. neoformans*. It was found that the apoptosis-inducing factor 1 (*AIF1*) is required for ALCD and that this phenomenon may function to rid cells exhibiting aneuploidy from the population (Semighini et al., 2011). Mutations of this gene result in the appearance of aneuploid subpopulations that have disomy of chromosome 1 and are highly resistant to Fluconazole. Such strains maintain Fluconazole resistance in absence of the drug. Because *AIF1* expression is downregulated in aneuploid cells obtained from clinical samples, it is thought that this gene may play a central role in maintaining correct ploidy within the population (Semighini et al., 2011).

Fungal Centromeres

The centromere is a specialized region of heterochromatin directly involved in ensuring the proper association of spindle microtubules with chromosomal DNA. Centromeres may be defined either as the primary site of constriction within a chromosome or as the chromosomal region containing a centromere-specific histone H3

variant. Only one functional centromere/microtubule attachment may exist in a fungal chromosome; more than one connection to the spindle apparatus results in breakage or improper segregation of chromosomes. If the centromere of a chromosome is unable to establish a faithful connection with the plus ends of spindle microtubules nondisjunction may result as both sister chromatids are ushered to the same pole of a dividing cell during anaphase (Stoler et al., 1995). Centromeres typically contain few genes, show little transcriptional activity, and rarely are sites for recombination (Roy and Sanyal, 2011). Centromeric length, as well as the sequences found within the centromere, varies greatly across fungal species. These are a rapidly evolving chromosomal region, potentially driving the divergences so far discovered and possibly expediting speciation. Many fungal species studied so far have "point centromeres", described as highly conserved sequences less than 400 bp in length. The *S. cerevisiae* point centromere is 125 bp long and is composed of three conserved sequences (CDE, centromere DNA element) found in every chromosome: CDEI, an 8 bp sequence required for efficient chromosome segregation; CDEII, a 78-86 bp AT-rich sequence, and CDEIII, a 25 bp imperfect palindrome with 7 invariant essential base pairs. CDEIII is known to be absolutely essential as single base pair mutations may completely abrogate functionality. Deletion of CDEI results in increased rates of chromosome missegregations while mutations in CDEII only have marginal effects (Roy and Sanyal, 2011). The length of repeat units seen in centromeres is somewhat conserved and approximately equal to the length of DNA thought to be in contact with centromeric DNA as it wraps around the histone complex (Roy and Sanyal, 2011).

The centromeres of other fungal species, by contrast, are much larger and less conserved. These are termed "regional centromeres" and are highly repetitive, with sizes ranging from 40 kb to several Mb. It is thought that epigenetic factors, including histone methylation and deacetylation, are more responsible for the formation of these centromeres as opposed to specific sequences (Verdaasdonk and Bloom, 2011). The centromeres of *Schizosaccharomyces pombe*, for example, range from 40 kb to 110 kb and contain an essential central core surrounded symmetrically on both sides by innermost repeats that are unique to each centromere and outermost repeats distal to the core. Centromeres are surrounded by facultative pericentric heterochromatin. In *S. pombe*, a direct relationship between RNA interference and centromere propagation and stability has been noted. Both strands of the outermost repeats are transcribed during S phase, activating the RNAi machinery. Deletion of genes involved in this process results in increased chromosome loss and revealed RNAi to be essential for centromeric heterochromatin maintenance (Dumesic et al., 2013).

Point centromeres are likely evolutionarily derived from regional centromeres, due to the facts that few species with point centromeres have been found and those that have been identified share a common ancestor that existed after regional centromeres appeared in Fungi (Meraldi et al., 2006). The centromere of *Candida albicans*, a species more closely related to *S. cerevisiae* than to *S. pombe*, is intermediate in size, usually composed of 4-18 kb. The centromere of *C. neoformans* has yet to be positively identified, with transposon-rich, gene-free 40-110 kb regions serving as putative regional centromeres (Loftus et al., 2005).

Fungal Kinetochores

Protein supercomplexes known as kinetochores assemble at the centromere of each chromosome to enable the interaction of centromeric DNA with the cellular components that exact these processes. The organization, sequence, and length of centromeric DNA and the individual proteins that compose the kinetochore vary greatly among yeasts; however, the overall structure of the kinetochore is widely conserved (Roy et al., 2011), with an "inner kinetochore" layer that associates directly with DNA, an "outer kinetochore" layer that attaches to the microtubules, and a "middle kinetochore" layer that links these two to coordinate their functions. Another example of this conserved structure is the presence of histone variants throughout the centromeric chromatin. These variants belong to the *CENP-A*/*CenH3* family and their restriction to the centromere is epigenetically regulated. This histone variant is accompanied at the kinetochore core by the *Mis12*/*Mtw1*, *NDC80*/*Hec1*, and *KNL1*/*SPC105* complexes, which create a site for spindle microtubule attachment, and the *Sim4*/*COMA* complex, another member of the middle kinetochore layer. Of these proteins, Mis12p/Mtw1p has been implicated as a scaffold protein in the linker layer, acting as a docking site for other kinetochore proteins.

Kinetochores in budding yeast are clustered into a single focus as opposed to being dispersed along with the chromosomes as in most other Eukaryotes. This has possible implications for the evolution of complex kinetochores such as those seen in vertebrate animals (Chan et. al., 2005). The kinetochore in budding yeast cells is composed of at least seven distinct protein complexes in fixed ratios that assemble in an ordered, hierarchical manner. One difference seen between the kinetochore structure of

S. cerevisiae and *S. pombe* is the number of microtubules attached to each kinetochore: in *S. cerevisiae* only one histone H3-variant containing nucleosome is found in the kinetochore, therefore only one spindle microtubule is found attached to each nucleosome. However, in *S. pombe* up to three variant nucleosomes may exist per kinetochore, allowing up to three microtubules to bind (Petrovic et al., 2010).

The Outer Kinetochore

The outer kinetochore consists of many proteins, of which the DASH complex, also known as the Dam1p-Duo1p complex, is of primary importance. The DASH complex is named for its components, which include Dam1p, Duo1p, and Dad1p (Duo1 and Dam1 interacting), Spc19p, Spc34p, and Ask1p/Dad2p in equimolar concentrations (Cheeseman et al., 2001). Both Dam1p and the entire Dam1 complex have been shown to bind microtubules in vitro (Cheeseman et al., 2001). A Dad2-GFP fusion protein yielded punctate localization along longer spindle fibers. All of these proteins were shown to associate with the centromere and kinetochore in *S. cerevisiae*. ts degron-tagged *DAD2* cells arrest mostly in the large budded stage with some cells displaying spindles that had broken down. Similar results have been obtained from ts –*dad1* mutants (Cheeseman et al., 2001).

The DASH complex has recently been shown to act as a heterodecamer, with each protein being essential for chromosomal attachment to the kinetochore and thereby viability in *S. cerevisiae* (Miranda et al., 2005). Each of the ten proteins that constitute this complex has been shown to be essential in ascomycetous species. Recombinant DASH can bind microtubules in vitro and appear as irregular striations perpendicular to the axis of the microtubule when imaged with electron microscopy. As the ends of these

striations could not be detected, it is thought that DASH either forms a ring around the microtubule or wraps around the microtubule in a helical fashion (Miranda 2005).

The Middle Kinetochore

The outer kinetochore is anchored to the inner kinetochore and ultimately the centromeric DNA through its associations with proteins of the middle kinetochore. In budding yeast, the KMN network comprises the core of this linker layer and is composed of three constituent protein complexes: KNL-1/Blinkin/Spc105p, the MIND complex, and the Ndc80 complex. The length of this network is long enough to span the entire outer kinetochore (Hornung et al., 2010). The MIND complex has a quaternary structure that forms a 25 nm long, bilobed structure that has been shown to interact with both Ndc80p and KNL-1/Blinkin/Spc105p, anchoring it within the KMN network (Hornung et al., 2010).

The MIND complex

As mentioned above, the MIND complex consists of four proteins: Nnf1p, Mtw1p, Dsn1p, and Nsl1p. *ScNNF1* (Necessary for Nuclear Function 1) encodes a 201 amino acid coiled-coil protein expressed in low abundance that was first isolated from nuclear envelope enriched fractions in *S. cerevisiae* (Euskirchen, 2002). All of the fungal Nnf1 proteins studied so far, in addition to vertebrate homologs, are roughly the same size (~ 200 aa) and feature a central coiled-coil domain (res. 60-100 and 120-175 in ScNnf1p, see Supplementary Figure 4) (Hornung et al, 2010). Temperature-sensitive mutants of *NNF1* resulted in cells that when grown at 37°C exhibited the large budded, uninucleate phenotype characteristic of cytokinetic mutants. Nuclei were stuck at the

mother-bud neck and DNA was distributed between the two daughter cells. Spindle morphology was aberrant as well, indicating Nnf1p is essential for spindle function and thus cell division. In order for the cell cycle to progress DNA must be distributed equally; this is dependent on correct positioning of the spindle apparatus in the bud neck during anaphase. Several genes were identified in this study that acted as dosage suppressors for mutant Nnf1p. Among these were *MTW1* and *DSN1* (Dosage Suppressor of *NNF1*). ScDsn1p is a 576 aa, 66 kDa protein whose expression peaks in G_2. A synthetic lethal screen was performed using ts-*nnf1* cells; this revealed synthetic lethality with both the *MTW1* gene and a new gene, *NSL1* (*NNF1* Synthetic Lethal 1), encoding a 216 aa, 25 kD protein. *MTW1*, *NSL1*, and *DSN1* were shown to be essential for spore germination and viability through tetrad analysis of mutant cells.

Fluorescence microscopy showed that the four MIND proteins in *S. cerevisiae* were each independently present as a single dot at the nuclear periphery in unbudded cell, as side-by-side dots in small-budded cells, and at opposite ends of the dividing nucleus in large-budded cells, behavior typical of spindle pole body or kinetochore proteins in yeast. Colocalization of MIND proteins was also observed. *DSN1* and *MTW1* are interaction suppressors of ts-*nnf1*; overexpressing these genes at restrictive conditions may prevent the degradation of the ts-*nnf1* protein by sequestering the unstable monomer. In addition, Dsn1p and Nsl1p were shown to interact in a yeast-two hybrid assay. It is thus thought that Nnf1p, Dsn1p, Mtw1p, and Nsl1p act as a subcomplex within the kinetochore (Euskirchen, 2002). Direct interaction between Mtw1p and the other MIND complex members was first demonstrated in pull-down experiments in *S. cerevisiae* using FLAG-tagged Mtw1p (de Wulf et al., 2003). Temperature-sensitive mutant strains of Nsl1p and

Dsn1p in *S. cerevisiae* have demonstrated gross mitotic defects, displaying cell-cycle arrest in the budding stages and spindle instability (Nekrasov et al., 2003).

More recent studies of the *S. cerevisiae* MIND complex by Hornung et al. (2010) and Maskell et al., 2010 revealed that Mtw1p, Nnf1p, Nsl1p, and Dsn1p are present in even stoichiometric proportions of 1:1:1:1. Unlike the *Ndc80* and *Dam1* complexes, MIND tetramers may form from the assembly of two stable heterodimers of Mtw1p with Nnf1p, the MN subcomplex, and Dsn1p with Nsl1p, the DN subcomplex. The MIND heterotetramer forms an elongated dumbbell-like structure 25 nm in length (Hornung et al., 2010). The DN subcomplex forms a 150 kDa lobe at one end while the MN subcomplex forms a 45 kDa coiled-coil lobe at the other end, with about 9 nm of linker between the two lobes. The Ndc80 complex binds to spindle microtubules through one of its two globular domains (Nuf2p) and to the MIND complex through the other (Spc24/25p) (Wei et al., 2007). For this latter association, the Spc24/25 domain of Ndc80 is proposed to bind the DN subcomplex of MIND. It has further been shown that the MIND complex coelutes with the Ndc80 complex and only copellets with microtubules in the presence of Ndc80. It is therefore thought that the association between the MIND complex and spindle microtubules is mediated through the Ndc80 complex.

NDC80 binds spindle microtubules through the globular domains of Ndc80p and Nuf2p. MIND overlaps part of NDC80 and acts as a bridge between outer and inner kinetochore layers. Analytical ultra centrifugation suggests the MN dimer is more elongated than the DN dimer. MIND complex is flexible and ~21 nm long with a globular 8 nm bilobal head and a 13 nm tail. It is likely that the tail structure is composed

of more than one coiled coil and is the connection point between the MIND complex and the inner kinetochore. All four proteins contribute to the head domain; the interface for tetramer formation between the four members is therefore believed to lie within the head's core. The head contains a large, structurally significant cavity likely involved in binding to the NDC80 complex. Nnf1p and Dsn1p are thought to extend the entire length of the complex, while Nsl1p is mostly contained to the head domain, with its C terminus just extending into the tail region. MIND also binds the Knl1p (as in KMN network) homolog ScSpc105p through conserved hydrophobic motifs in carboxy-terminal region. This reaction is probably mediated through the C terminus of Nsl1p (Maskell et al., 2010). These results are largely in agreement with similar experiments performed on the human MIS12 complex (Petrovic et al., 2010). As the MIND complex has been shown to interact with the Ndc80 complex, it is thought that MIND acts to bridge the gap between the microtubule-binding components and the centromeric DNA (Hornung et al., 2011). Of the proteins in this network, Mtw1p acts to maintain correct centromere/kinetochore structure, making it essential for proper segregation of chromosomes, and has been characterized in many diverse organisms, from nematodes to humans.

The Inner Kinetochore

The inner kinetochore serves as the connection between centromeric DNA and the rest of the kinetochore superstructure. Proteins of the inner kinetochore are highly conserved from yeast to metazoans (Westermann et al., 2003). ChIP analysis followed by tandem affinity purification has been used to demonstrate the association of both Cse4p and Mif2p with centromeric DNA, along with the MIND complex members Nnf1p, Nsl1p, and Dsn1p (Westermann et al., 2003). Through this method it was also

found that MIND copurifies with the Ctf19 complex. As no other nucleosomal proteins copurified with MIND it may be assumed that the Ctf19 complex is distal to the centromere as compared to Mif2p (Westermann et al., 2003).

MIF2

MIF2 (Mitotic Fidelity 2) is the budding yeast homolog of mammalian CENP-C, with high homology within two conserved carboxy-terminal regions (Meluh and Koshland, 2003). *MIF2* was originally identified in *S. cerevisiae* through aberrant effects on chromosome transmission of an overexpressed fragment and was shown to be essential for chromosome segregation in this species with loss of this protein yielding mitotic delay (Meeks-Wagner et al., 1986). The Mif2 protein has an acidic domain and a proline-rich A-T hook through which it interacts with DNA. Significant increases in minichromosome loss have been shown in ts-*mif2* mutants alone and in conjunction with CDEI-defective minichromosomes but not those defective for CDE-II or CDE-III (Meluh and Koshland, 1995). A lethal phenotype is also obtained when *MIF2* is mutated along with *CEP1*, whose product has been found at CDE-I. These synthetic phenotypes indicated a role for Mif2p in centromere function. Mif2p has also been copurified with both Mtw1p and Cse4p.

Mif2p and the MIND complex depend on each other for centromeric localization: temperature sensitive mutants of MIND members Mtw1p and Nnf1p (along with Cse4p) yielded diminished Mif2p signal at the centromere under restrictive conditions. Additionally, Mtw1p showed reduced ChIP signal when a temperature-sensitive (ts)-*mif2* strain was cultured under restrictive temperature, suggesting an interdependency between

these proteins for proper localization (Westermann et al., 2003). Similar experiments showed that the presence of the Ndc80 complex at the kinetochore is diminished in ts-*nnf1* cells under restrictive conditions while Nnf1p and Mtw1p do not depend on Ndc80 for centromeric localization (Westermann et al., 2003).

All three layers of the kinetochore are subject to regulation by phosphorylation. The Aurora kinase Ipl1p has been shown to phosphorylate Ndc80p, Dam1p, Mif2p and Dsn1p *in vitro* (Westermann et al., 2003). This is essential for proper function in Mif2p, as evidenced by the lethal phenotype achieved by mutating two serine residues known to be phosphorylated *in vivo* to alanine. This contrasts with the phosphomimetic mutation of these serine residues to aspartic acid, which only yielded slower growth at 37° (Westermann et al., 2003). In addition to positive regulation controlled by protein kinases, protein phosphatases play a crucial role in kinetochore function. One such enzyme, PpeI, has been shown to have an essential role in Mis12p function in *S. pombe*; PpeI (or its bound partner Ekc1) is known to dephosphorylate the Mis12p protein and mutations in the *PPEI* gene result in missegregation of chromosomes in dividing cells (Goshima et al., 2003).

CSE4

CSE4 is the budding yeast homolog of mammalian CENP-A, a histone H3 centromeric variant (Westermann et al., 2003) that through mass spectrometry has been shown to completely replace histone H3 at the centromere. The CENP-A homolog in *Candida albicans*, CaCse4p, has been shown to be required for centromere chromatin formation and its presence has been shown to induce a non-canonical chromatin structure (Roy et al., 2011). *CSE4* was first isolated through an EMS mutagenesis screen to

identify mitotic chromosome segregation mutants. Mutant cells showed a recessive ts phenotype and increased mis-segregation of chromosomes. These cells also arrested in the large-budded state with the nucleus near the bud neck and shortened spindles (Stoler et al., 1995). An essential role in cell division for *ScCSE4p* was demonstrated through tetrad analysis. The carboxy terminus of *CSE4* shares homology with the hydrophobic histone-fold domain of histone H3; however the amino terminus of ScCse4p is 94 amino acids longer than that of histone H3 (Stoler et al., 1995). ScCse4p was first demonstrated to have a role in nucleosome formation through increased nuclease sensitivity while expressing a ts mutant at the restrictive temperature. This study also revealed localization patterns through the cell cycle similar to that of the spindle pole bodies, confirming chromosomal localization (Meluh et al., 1998). It is believed that the specialized centromeric nucleosome functions as a scaffold for the hierarchical assembly of kinetochore components required for chromosome segregation, especially those at the inner kinetochore such as Mif2p (Westermann et al., 2003).

Cse4p interacts with the CDE-II portion of the centromere (Verdaasdonk and Bloom, 2011). Wrapping of CEN DNA around the non-canonical histone explains genetic interactions between proteins bound to CDE-I and CDE-III. The amino terminus of Cse4p is hypervariable between most species, likely due to differences in quickly evolving centromeric sequences. Cse4p has a carboxy-terminal Histone Fold Domain (HFD) shared by all histones (Roy and Sanyal, 2011). Complete loss of Cse4p (Chromosome segregation 4) is lethal in every organism studied (Verdaasdonk and Bloom, 2011). Cse4p is regulated by Scm3p, which is responsible for recruitment of

Cse4p to centromeric nucleosomes during S to G_2 phase, and Psh1p, an E3 ubiquitin ligase that removes mis-incorporated Cse4p from extra-centromeric nucleosomes.

COMA

The Ctf19 complex is the budding yeast homolog of CCAN (Constitutive centromere-Associated Network) of higher eukaryotes and contains at least 11 proteins organized into stable subunits. Among these, the COMA subcomplex is at the core of the Ctf19 complex and includes *Ctf19, Okp1, Mcm21,* and *Ame1* in a 1:1:1:1 stoichiometry. The COMA complex has also been shown to coelute with the MIND complex (Hornung et al, 2010). This association has been shown to occur at a site on the MIND complex different from that of the binding site of Ndc80. It is therefore thought that the COMA complex is responsible for the localization of the MIND complex to the inner centromere. The MIND complex is thought to bind COMA through the MN subcomplex, with Nnf1p being the most centromere proximal (Hornung et al., 2010).

The Role of *MTW1*

Temperature-sensitive mutants of MIND complex subunits have revealed that this complex is necessary for the biorientation of kinetochores and the segregation of chromosomes. One such mutation was discovered in the fission yeast (*Schizosaccharomyces pombe*) that prevented cells from growing above 36°C (Goshima et al., 1999). It was found that SpMis12p is a 30-kD protein essential for viability due to its prominent role in the segregation of chromosomes via the regulation of spindle length during mitotic anaphase. The mutant discovered had an amino acid substitution of glycine to glutamic acid at the fifty-third residue of the conserved amino terminal region.

This idea is supported by the finding that missegregations in mutated cells lead to aneuploidy, a common cause of non-viability. This homolog was found using fluorescent colocalization with mitotic tubulin to localize at the centromere throughout the cell cycle (Goshima et al., 1999). As the effect of growth above the inhibitory temperature in either of the gap phases of the cell cycle is delayed until the following mitotic division, it was thought that Mis12p also contributes to mitosis by setting up centromere structure for the following M phase. This step has also been correlated with sister chromosome cohesion in that chromosomes *mis12* mutant cells do not segregate correctly. Studies performed using gene disruptions have shown a cell cycle phenotype with a large bud and the nucleus usually located in the neck between the two daughter cells. These results imply that *MTW1* is required for cell viability in ascomycetous species. The fact that the daughter cells were developed to this stage implies that this mutation does not activate the spindle checkpoint. The results of this study imply that centromere proteins regulate the correct morphogenesis of the mitotic spindle.

Another temperature-sensitive kinetochore mutant was later described in the budding yeast *Saccharomyces cerevisiae*. The mutation responsible for this phenotype was found to be in the budding yeast *MTW1* (*Mis twelve*-like protein) gene (Goshima and Yanagida, 2000). Two notable differences exist between the centromeres and kinetochores of *S. pombe* and *S. cerevisiae*; one difference is that the centromeres of *S. pombe* chromosomes are one hundred times larger than those seen in the chromosomes of *S. cerevisiae*. This is true despite the fact that the genomes of the two species are approximately equal in size (14.1 Mb in *S. pombe* vs. 12.2 Mb in *S. cerevisiae*). *S. pombe* has three chromosomes compared to sixteen seen in *S. cerevisiae*; however this

difference in the number of chromosomes, and thus centromeres, is not enough to account for the discrepancy seen in total centromeric DNA (Goshima and Yanagida, 2000). Another difference between the two species is that the spindle forms during mitosis in *S. pombe*, while in *S. cerevisiae* spindle formation can be observed earlier in the cell cycle at the first gap phase. This might affect the length of the second gap phase as early spindle assembly may shorten the time required for the cell to set up its division machinery. Another study showed that in *S. cerevisiae* the sister centromeric DNA regions were separated at the time of spindle formation; however, the arms of the chromosomes were found to remain associated during this time. It was hypothesized that this association may aid in generating the opposing force against the pull of spindle microtubules (Goshima and Yanagida, 2000). This study used a mutant *MTW1* with the same functional mutation seen in *S. pombe*: a substitution of glutamic acid instead of glycine at sixty-fourth amino acid. This mutation resulted in a temperature sensitive phenotype at 36°C. Cells transformed with this mutated *MTW1* underwent S phase of the cell cycle but were found to arrest during M phase with a large bud, a short spindle, and a single nucleus between the cell and the bud. By staining nuclei with DAPI and microtubules with GFP and performing nuclear bud counts it was found that that these cells create metaphase spindles that are longer than those seen in wild type cells (Goshima and Yanagida, 2000).

A more recent study on the *Candida albicans* homolog of *MTW1* indicated a similar role for this gene in a third yeast species. It was found that *MTW1* is essential for viability in *C. albicans* and that mutation of the highly conserved glycine residue resulted in yet another temperature-sensitive phenotype (Roy et al., 2011). These cells showed

the G_2/M phase arrest along with chromosome missegregation typical of *MTW1* mutants. Another approach used in this study was the use of a promoter-swap construct in which the endogenous *CaMTW1* promoter was replaced with the *CaPCK1* promoter. This promoter induces transcription in the presence of succinate and represses expression in the presence of glucose, permitting conditional expression of the downstream gene. Growth of these cells in glucose media yielded the same phenotype as the ts mutant and a lack of viability, demonstrating an essential role for this gene in cell cycle progression for *C. albicans* (Roy et al., 2011). Another intriguing finding of this study was a strong codependence for centromere localization between CaCse4 and CaMtw1. Such a relationship was also noted for CaMif2 and CaMtw1 (Roy et al., 2011).

Although outer kinetochore proteins such as Mtw1p have been previously described in other fungal species such as *S. pombe, S. cerevisiae,* and *C. albicans*, such work has yet to be performed in the more pathogenic species *C. neoformans*. The previously studied species are all ascomycetes whereas *C. neoformans* is a badsidiomycete. It is therefore unknown if CnMtw1p plays the same role in kinetochore structure and function as that of its identified homologs in other fungal species. *C. neoformans* differs from those aforementioned species, however, in that medical complications due to this species have risen dramatically in recent decades. This rapid increase in infection rate is tightly associated with the advent of HIV/AIDS and the role of *C. neoformans* as an opportunistic pathogen. At the peak of this epidemic, approximately 10% of AIDS patients developed cryptococcosis (Casadevall and Perfect, 1998). Establishing the fundamental role of this protein in kinetochore structure and its necessity for proper function may provide a potential target for future therapeutic

treatments. To begin demystifying the cryptococcal kinetochore, this study seeks to determine whether *MTW1* plays a homologous role in *C. neoformans* as it does in the ascomycetous species through mutational analysis and conditional expression of the mRNA transcript and protein. Additionally, the identity and essentiality of several other putative kinetochore homologs are determined in conjunction with *CnMTW1*.

MATERIALS AND METHODS

Strains Used

KN99α (IBCN2) was used as a wild type control for growth and morphological experiments. *MTW1-mCh-Neo* #11 (IBCN20), containing the *mCherry* fluorescent protein gene downstream of the *MTW1* coding sequence and the neomycin resistance marker (NEO^R) was used as the starting strain for creating the temperature sensitive *mtw1* mutation and the P_{CTR4}-*MTW1-mCherry* strains.

JEC21 (IBCN43) was used for all RNAi experiments as both the source material for genomic inserts of targeted genes and for the RNAi vector transformations and growth assay.

Media and Growth Conditions

All *C. neoformans* strains were maintained in YPD media (1% yeast extract, 2% tryptone, and 2% dextrose) at 30˚C. For selection of transformants, YPD media was supplemented with various antimicrobial agents including neomycin (G418, Fisher BioReagents BP673) at 100 µg/mL and hygromycin (EMD Millipore 400051-1MU) at 350 µg/mL. Biolistic transformations were carried out on YPD plates containing 1M sorbitol before transferring to the appropriate selective medium.

YPD/Neo plates containing 200 µM bathocuproine disulfonic acid (BCS) (Sigma-Aldrich) and $CuSO_4$ at concentrations of 25 µM and 50 µM were made to test P_{CTR4}-*MTW1* transformants. For RNAi experiments, YPGal medium (which contains 2%

galactose in lieu of dextrose) or YPGal medium supplemented with 1 mg/mL 5-fluoroorotic acid (5-FOA) (US Biological) were used.

Liquid LB media containing 0.5% yeast extract, 1% tryptone, and 1% NaCl was used for overnight cultures of *E. coli*. Agar plates were made using LB media supplemented with 100 µg/mL ampicillin for selection of cells containing the desired plasmids. SOC medium (2% vegetable peptone, 0.5% yeast extract, 10 mM NaCl, 2.5 mM KCl, 10 mM $MgCl_2$, 10 mM $MgSO_4$, 20 mM Glucose) was used for outgrowth in bacterial transformations.

Identification of Kinetochore Genes in *Cryptococcus*

Putative homologs for kinetochore genes previously studied in ascomycetous species were identified through a search performed using the Domain Enhanced Lookup Time Accelerated (DELTA) protein BLAST tool available from NCBI (Boratyn et al., 2012). The amino acid sequences obtained through this search were then used to identify the nucleotide sequences that code for these proteins in the *C. neoformans* genome.

Protein Sequence Comparisons

Protein sequences for kinetochore homologs were found using DELTA-BLAST and their accession numbers were submitted to the multiple pair-wise sequence analysis tool COBALT (Papadopoulos and Agarwala, 2007). The results of this alignment were graphically represented using ESPript 2.2 (Gouet et al., 1999). Global sequence comparison of each protein with its fungal homologs was performed using EMBOSS

Needle whereas local regions of sequence similarity were described using EMBOSS Water (Rice et al., 2000).

Genomic DNA Preparation

Genomic DNA was prepared as described in Bose and Doering (2011). Briefly, cells grown overnight in YPD at 30˚C were harvested by centrifugation at >12,000 g. The cells were lysed in extraction buffer (50 mM Tris-HCl, pH 8; 20 mm EDTA; 1% SDS) by vortexing 25 minutes in 5 minute intervals with glass beads with 3 minute intermittent incubations on ice, treated with 30% polyethylene glycol and 5 M NaCl, and precipitated in ethanol. The genomic DNA was then treated with RNase to remove RNA contaminants and resuspended in 50 µL sterile dH_2O.

Construction of RNAi Vectors for Kinetochore Genes

Regions of each of the putative homologs of kinetochore genes, ranging from 272 bp for *NSL1* to 404 bp for *NNF1* were amplified from the *Cryptococcus* genome (JEC21 strain) using polymerase chain reaction (PCR). These reactions were carried out using forward and reverse primers as designated in Table 1 and annealing temperatures for each reaction, respectively. These reactions had the following conditions: 98°C 30 s; 30 x (10 s 98°C, 10 s (see Table 1)°C, 45 s 72°C); 5 min. 72°C. Each reaction containing 29.5 µL dH_2O, 10 µL 5X HF polymerase buffer, 4 µL dNTPs, 2.5 µL of each primer, 0.5 mL Phusion® Taq polymerase (NEB), and 1.0 mL of JEC21 gDNA as template for a final volume of 50 µL.

The products of these reactions were column-purified using the Wizard® SV Gel and PCR Clean-Up System (Promega). Ten microliters of each of the purified fragments was digested with 2 µL of either SpeI or NdeI restriction enzyme (NEB) in a final volume of 50 µl for 4 hours at 37˚C, followed by heat inactivation for 20 minutes at 80°C. The pIBB103 RNAi vector (Figure 18) was subjected to the same restriction digest as the amplified gene fragment and treated with 1 µL CIP at 37°C for one hour to remove 5' phosphate groups from the ends thereby preventing the opportunity for self-ligation of the vector without the desired gene insert.

The digested fragments were ligated into the appropriately digested pIBB103 using 2 µL each of the digested insert and vector and 1 µL of T4 DNA ligase (NEB) in a 15 µL total volume. A control ligation of the pIBB103 vector by itself was also performed.

Bacterial Transformation and Plasmid Preparation

50 µL of NEB 5-alpha high efficiency competent *E. coli* cells (#C29871) was used for transformation per sample. Briefly, 7 µl of each ligation product was added to the cells, incubated on ice for 30 minutes, and heat shocked at 42°C for 30 seconds, followed by a 5 minute incubation on ice. The cells recovered for 1 hour at 37˚C in 250 µl SOC medium, plated on a selective medium (LB/Amp), and allowed to grow overnight at 37°C. Transformants from these plates were grown overnight in liquid LB/Amp and plasmids extracted using the Wizard® Plus SV Minipreps DNA Purification System protocol (Promega).

Table 1. Primers used for RNAi. Restriction sites are shown in red text. Homologous sequences are in uppercase while non-homologous adaptor sequences are in lowercase.

Name	Description	Sequence (5' to 3')	Tm (°C), Phusion	Annealing Temp (°C)	Amplicon Length (bp)	Restriction Enzyme
BLO47	*MTW1* RNAi S	ccggttaCTAGTTCCAGCAAGATTACG	57.0	57.0	343	SpeI
BLO48	*MTW1* RNAi AS	ccggttactagTAGATTTAGAATCCTTCGCTAC	56.0			
BLO58	*DAD1* RNAi S	cggttactAGTCTTTCTTCGAGAGGGAA	60.1	61.0	383	SpeI
BLO59	*DAD1* RNAi AS	cggttactAGTTTGCACCTCCTGTACCA	62.7			
BLO60	*DAD2* RNAi S	ggttcATATGCCGGTCTTCAGGCTT	65.0	65.0	350	NdeI
BLO61	*DAD2* RNAi AS	ggttcaTATGCTAAGCGCACGAGACA	65.0			
BLO62	*CSE4* RNAi S	ggttactAGTAACGAGCCCAAGTCGAG	63.7	61.0	360	SpeI
BLO63	*CSE4* RNAi AS	ccggaaactAGTTTGGCAATCAACAAATC	59.6			
BLO64	*MIF2* RNAi S	ccggttactAGTACTTATTCCCGCGCGGA	67.9	65.0	330	SpeI
BLO65	*MIF2* RNAi AS	ccggttactaGTCTGACAGAAGGAGAGGGG	63.3			
BLO68	*NNF1* RNAi S	ccggttactagtAAGGCAATGGAGAATGCCTG	66.6	68.0	404	SpeI
BLO69	*NNF1* RNAi AS	ggccaactaGTCCCTCAACCTCTCATATGTCTCATC	68.0			
BLO70	*NSL1* RNAi S	ccggttactagTCCCAGCCTTTGTCTCATTTGA	68.1	68.0	278	SpeI
BLO71	*NSL1* RNAi AS	ggccaaactAGTACTTTGGCTCCAGGCGACTT	68.3			
BLO72	*DSN1* RNAi S	ccggttactaGTTTCGTGAGAAAGACGCGAAAG	68.2	68.0	329	SpeI
BLO73	*DSN1* RNAi AS	ccggaaactagTCGGGTCAGGATATGCCGTAG	68.3			

Transformation of *Cryptococcus* by Electroporation

20 µl of plasmids to be transformed into *Cryptococcus* were digested using 6 µl I-SceI (NEB), and column purified using the Wizard® SV Gel and PCR Clean-Up System (Promega). Electroporation was performed as described in Bose, 2004. Briefly, JEC21 cells were grown in YPD medium to the desired concentration (10^7 cells/mL). The cells were harvested by centrifugation at 3000 x g, washed twice with chilled distilled water, once with chilled electroporation buffer (10 mm Tris-HCl, pH 7.5, 1 mm $MgCl_2$, 270 mM sucrose), and treated with 1M DTT for 10 minutes to reduce disulfide bonds. The cells were resuspended in residual buffer for electroporation. Five microliters of each purified digested plasmid were used to electroporate 50 µL of the cells using the following settings: 500 volts, 25 µF capacitance, and infinite resistance. A negative control consisting of cells electroporated without the addition of any DNA was also prepared. The electroporated cells were allowed to grow in 1 mL YPD medium at 30°C for 3 hours before 500 µL of each sample was plated on both YPD/Neo and YPGal/Neo media and incubated for 3 days at 30°C.

Generation of ts-*mtw1* Construct / Mutagenic Overlap PCR

Creation of ts Overlap Templates

Overlap PCR was chosen as the best strategy for creating the desired construct because its use has been successful in previous studies on *C. neoformans*. Also, overlap PCR is a more versatile method than molecular cloning and can more consistently generate DNA fragments long enough for efficient homologous recombination in *C. neoformans* (Davidson et al., 2002). Initial reactions were performed to generate the two

DNA templates for the final overlap PCR that would each contain the desired mutation. The primers designed for this experiment are listed in Table 2. To generate the 5' fragment a PCR was run using BLO23 as the forward primer and BLO32 as the reverse primer with the following conditions: 100°C lid; 98°C 30 s; 30 x (10 s 98°C, 10 s 70.0°C, 45 s 72°C); 5 min. 72°C; 4°C hold. The 3' fragment was generated from a similar PCR using BLO31 as the forward primer and BLO30 as the reverse primer: 100°C lid; 98°C 30 s; 30 x (10 s 98°C, 10 s 69.0°C, 2.5 min. 72°C); 5 min. 72°C; 4°C hold. These PCRs were performed in triplicate with each reaction containing 29.5 mL dH_2O, 10 mL 5X HF polymerase buffer, 4 mL dNTPs, 2.5 mL of each primer, 0.5 mL Phusion Taq polymerase, and 1.0 mL of *MTW1-mCh-Neo* #20 gDNA as template for a final volume of 50 µL. The products of these PCRs were gel purified for examination on an agarose gel to confirm that the desired product was made.

ts Overlap PCR

Overlap PCRs were set up using the above purified upstream and downstream fragments as templates and BLO24 and BLO29 as forward and reverse primers, respectively, with the following conditions: 100°C lid; 98°C 30 s; 30 x (10 s 98°C, 10 s 67.0°C, 3.0 min. 72°C); 5 min. 72°C; 4°C hold. This reaction was performed in triplicate with each reaction containing 28.5 mL dH_2O, 10 mL 5X HF polymerase buffer, 4 mL dNTPs, 2.5 mL of each primer, 1.0 mL Phusion Taq polymerase, 0.5 mL of the purified upstream overlap template and 1.0 mL of the purified downstream overlap template for a final volume of 50 µL. Overlap products were then gel purified and pooled in 40.0 µL dH_2O. Isolation of the desired product was confirmed by gel electrophoresis.

Generation of P_{CTR4} Overlap Constructs / Promoter Swap Overlap PCR

In contrast with the ts mutagenic overlap PCR strategy, the promoter swap construct requires the generation of three template pieces to be used in the overlap PCR. Two different versions of the *CTR4* promoter complex were used: the native P_{CTR4} promoter alone and P_{CTR4}*-2*, a variant composed of two copies of the promoter in tandem. The P_{CTR4}*-2* variant is approximately 250 bp larger than the single P_{CTR4} sequence.

Creation of P_{CTR4} Overlap Templates

To generate the 5' upstream fragment, a PCR was assembled using 29.5 µL dH_2O, 10 µL 5X HF polymerase buffer, 4 µL dNTPs, 2.5 µL of BLO23 as the forward primer, 2.5 µL of BLO26 as the reverse primer, 0.5 µL Phusion Taq polymerase, and 1.0 µL of *MTW1-mCh-Neo* #20 gDNA for a final volume of 50 µL. This reaction was run with the following conditions: 100°C lid; 98°C 30 s; 30 x (10 s 98°C, 10 s 67.0°C, 1.5 min. 72°C); 5 min. 72°C; 4°C hold. To make the 3' downstream fragment, 29.5 µL dH_2O, 10 µL 5X HF polymerase buffer, 4 µL dNTPs, 2.5 µL of BLO27 as the forward primer, 2.5 µL of BLO30 as the reverse primer, 0.5 µL Phusion Taq polymerase, and 1.0 µL of *MTW1-mCh-Neo* #20 gDNA, a final volume of 50 µL, were combined to run a PCR with conditions as follows: 100°C lid; 98°C 30 s; 30 x (10 s 98°C, 10 s 67.0°C, 3 min. 72°C); 5 min. 72°C; 4°C hold.

To create amplicons of the two *CTR4* promoters with flanks homologous to the *MTW1* 5'UTR immediately upstream of the start codon and the *MTW1* coding sequence beginning with the start codon, a PCR was run using 29.5 µL dH_2O, 10 µL 5X HF

polymerase buffer, 4 µL dNTPs, 2.5 µL of BLO25 as the forward primer, 2.5 µL of BLO28 as the reverse primer, 0.5 µL Phusion Taq polymerase, and 1.0 µL of the either the P_{CTR4} or P_{CTR4}-*2* plasmid preps as template for a final volume of 50 µL. These reactions were run with the following conditions: 100°C lid; 98°C 30 s; 30 x (10 s 98°C, 10 s 66.0°C, 1 min. 72°C); 5 min. 72°C; 4°C hold.

The products made by these reactions were confirmed by gel electrophoresis. These four PCRs were preformed in triplicate. Their products were gel purified and each pooled in 40 µL dH_2O.

<u>P_{CTR4} Overlap PCRs</u>

The final P_{CTR4} and P_{CTR4}-*2* overlap constructs were generated in two separate three piece overlap PCRs. Each reaction contained 28.0 µL dH_2O, 10 µL 5X HF polymerase buffer, 4 µL dNTPs, 2.5 µL of BLO24 as the forward primer, 2.5 µL of BLO29 as the reverse primer, 1.0 µL Phusion Taq polymerase, along with 0.5 µL of the purified 5' UTR fragment, 0.5 µL of either the purified P_{CTR4} or P_{CTR4}-*2* plasmid preps, and 1.0 µL of the purified 3' downstream fragment as templates for a final volume of 50 µL. Each of these two PCRs was performed under the following conditions: 100°C lid; 98°C 30 s; 30 x (10 s 98°C, 10 s 66.0°C, 4 min. 72°C); 10 min. 72°C; 4°C hold. These reactions were performed in triplicate. These products were gel purified in 40 µL dH_2O each and examined by gel electrophoresis.

Table 2. Primers used to create and study conditional *CnMTW1* mutants. For BLO25 through BLO28, orange text indicates homology to P_{CTR4} sequences. For BLO31 and BLO32, red text indicates the temperature sensitive mutant sequence.

Name	Description	Sequence (5' to 3')	Tm (°C), Phusion
BLO23	5' outer	CATCAGCAAAGTTGCCCTGACATA	69
BLO24	5' inner	TATGGGAAGACATTGTGCATAGCA	67
BLO25	*MTW1* 5' UTR – P_{CTR4} S	AGCAGCAGTCACCAGGACCAATTGGATATTGCTGTTTC	63.5
BLO26	*MTW1* 5' UTR – P_{CTR4} AS	AATATCCAATTGGTCCTGGTGACTGCTGCTTGGAAG	67.6
BLO27	P_{CTR4} – *MTW1* ORF S	GACAACGACTTCACCAATCATGGTCCCGAGGAAGCCAG	69
BLO28	P_{CTR4} – *MTW1* ORF AS	CTTCCTCGGGACCATGATTGGTGAAGTCGTTGTCG	63.7
BLO29	3' inner	GGTCGACCACAAGGTTCTGAATAT	66
BLO30	3' outer	CGCCAACGAGATTGAGAGAATATT	66
BLO31	*MTW1* ts mutant S	GATTTGTCATTCTAGG**AA**CTGCATGCTTTAGAAAC	72
BLO32	*MTW1* ts mutant AS	GTTTCTAAAGCATGCAG**TT**CCTAGAATGACAAATC	72
BLO45	*mCHERRY* AS	CACCCTTGGTCACCTTCAGC	67.3
BLO46	NEO^R S	GGATCTCGTCGTGACCCATG	68.3

Biolistics

Transformation of the overlap constructs was performed biolistically due to the low efficiency and mitotic errors associated with previous methods involving electroporation (Toffaletti et al., 1993). Biolistic transformation of wild type KN99α cells was performed using the purified overlap constructs as adapted from Davidson et al., 2000. Briefly, 50 mL of YPD culture was spun down for 5 minutes at 4,000 rpm (> 2600 g), 10°C. Pellets were resuspended in 5ml distilled water per 1ml cell pellet. 300 µL of this suspension was spread per 1M sorbitol YPD plate.

Gold Microcarrier Preparation: 250 mg of 0.6 µm gold beads (Bio-Rad) were washed once in dH_2O, followed by a wash in 1 mL of 100% ethanol. This was divided into four aliquots of 250 µL, each of which was diluted to 1 mL by the addition of 100% ethanol.

DNA Preparation: Forceps were used to submerge 2.5 cm orange discs in 100% ethanol, which were then allowed to dry. The gold beads were vortexed before being aliquoted in 10 µL each. To these aliquots were added 2 µL 1M spermidine (as a polyamine DNA carrier), 10 µL 2.5M $CaCl_2$, and 2 µL of the DNA construct to be integrated. These samples were vortexed and incubated at room temperature for five minutes with occasional flicking. Samples were then centrifuged at 13,000 rpm for 1 minute. The resulting supernatant was removed by pipet and the beads were resuspended in 600 µL of 100% ethanol by vortexing. Samples were spun down again at 13,000 rpm for one minute and resuspended in 6 µL by vortexing. These suspensions were then transferred by pipet to the 1 cm circle in the center of the biolistics disc. Ethanol on the discs was allowed to evaporate. These discs were inserted in the Bio-Rad PDS biolistics

machine one at a time, shooting each sample at a pressure of 2200 psi at cells spread on 1M sorbitol plates. Six hours later, 500 µL of sterile dH_2O was spread on each plate. A cell scraper (paint can lid remover) was used to scrape cells to the bottom of the plate while holding the plate at an angle. Cells were pipeted from here onto YPD/Neo plates (and YPD/BCS plates for P_{CTR4} transformants) and spread with glass beads.

Molecular Diagnostics of Putative Transformants

Strains previously identified as potentially containing the mutated version of *MTW1* were grown overnight in 3 mL YPD at 23°C. Genomic DNA samples of each strain were then prepared as previously described. To determine whether the entire insert had been completely integrated into the correct locus within the transformants' genomes, PCRs were performed using the gDNA samples as templates with BLO24 as the forward primer and BLO29 as the reverse primer; these primers lie immediately outside the region of interest and will thus amplify either the native sequence or the larger mutational sequence containing the *mCherry-NEO*^{R} construct. Conditions for this set of PCRs were: 100°C lid; 98°C 30 s; 30 x (10 s 98°C, 10 s 67.0°C, 3.5 min. 72°C); 5 min. 72°C; 4°C hold. These reactions were performed using 16 µL dH_2O, 2.5 µL 10X polymerase buffer, 1.25 µL $MgCl_2$, 2 µL dNTPs, 1.25 µL of BLO23 as the forward primer, 1.25 µL of BLO30 as the reverse primer, 0.25 µL NovaTaq polymerase, and 0.5 µL of gDNA from either KN99α, *MTW1-mCh-Neo* #20, 1.21, 1.28, 2.16, or 3.18.

Additional PCRs were performed off of these gDNA samples using one primer with homology within the construct and one primer homologous to sequences found in the genome only just outside the insert construct region. The two primers within the

construct bind to sites in the *NEO*^{R} sense strand and the *mCherry* anti-sense strand such that fragments from each end of the construct could be made. Such PCRs were performed for both the 5' upstream region and the 3' downstream region to confirm that the entire construct was present. The conditions for the 5' upstream region were: 100°C lid; 98°C 30 s; 30 x (10 s 98°C, 10 s 58°C, 3 min 72°C); 5 min 72°C; 4°C hold. This set of reactions were performed using 16 µL dH_2O, 2.5 µL 10X polymerase buffer, 1.25 µL $MgCl_2$, 2 µL dNTPs, 1.25 µL of BLO23 as the forward primer, 1.25 µL of BLO45 as the reverse primer, 0.25 µL NovaTaq polymerase, and 0.5 µL of gDNA from either KN99α, *MTW1-mCh-Neo* #20, 1.21, 1.28, 2.16, or 3.18. Conditions for the 3' downstream region were: 100°C lid; 98°C 30 s; 30 x (10 s 98°C, 10 s 59°C, 3 min 72°C); 10 min 72°C; 4°C hold, using BLO46 as the forward primer and BLO29 as the reverse primer. PCR products from these three sets of reactions were examined by gel electrophoresis to confirm the presence of the insert.

In order to determine whether the cells that arose from the biolistic transformation with the P_{CTR4} promoter swap overlap constructs contained the entire construct, PCRs were run using 16.0 µL dH_2O, 2.5 µL 10X polymerase buffer (500 mM KCl, 100 mM TRIS-HCl pH 8.8, 1% Triton® X-100), 1.25 µL 25 mM $MgCl_2$, 2.0 µL dNTPs, 1.25 µL each of BLO24 as the forward primer and BLO28 as the reverse primer, 0.25 µL NovaTaq polymerase, and 0.5 µL gDNA from each transformant strain. PCRs were run with the following conditions: 100°C lid; 98°C 30 s; 30 x (10 s 98°C, 10 s 67.0°C, 6 min. 72°C); 10 min. 72°C; 4°C hold.

Characterization of Mutant Phenotypes

Growth on solid media

Initial growth analysis was performed on YPD plates. Transformant strains were streaked out at three different temperatures: 23°C, 30°C, and 37°C. KN99α was streaked on each plate as a control. Plates were checked daily for the presence or absence of growth under the different conditions. Strains confirmed as mutants through molecular diagnostics, along with KN99α and IBCN#20 as controls, were streaked for single colonies on YPD at 23°C, 30°C, and 37°C.

Growth in liquid media

Overnight cultures of KN99α, G109D, and G109E were grown at room temperature (23°C). These cultures were used to inoculate 10 mL YPD cultures. These cultures were allowed to grow at room temperature for three hours before being split into three 3 mL cultures, one of which was incubated at 23°C, 30°C, and 37°C. Half-milliliter aliquots were saved at various time points up to three days. Growth was assessed by a combination of hemocytometry and optical density at 600 nm.

Microscopic Assessment

After growth measurements, samples were preserved in 10% formaldehyde for morphological analysis. The budding state distribution of each population was assessed by microscopic examination. Cells were scored as unbudded, small budded, medium budded, large budded, or mutant with at least 150 cells scored for each sample. DAPI staining of nuclei was achieved by permeablizing cells in PBS (8 g/L NaCl, 0.2 g/L KCl,

1.78 g/L $Na_2HPO_4 \cdot 2H_2O$, 0.27 g/L KH_2PO_4, pH 7.4) with 1% Triton-X-100 for 5 minutes at room temperature followed by 30 minutes incubation in 143 µM DAPI. Differential interference contrast and fluorescent images were obtained on a Nikon TE-2000 microscope.

ts Spot Assays

Strains were grown in liquid media overnight before being diluted with YPD to the desired concentration of approximately 3125 cells/µL. A five-fold dilution series was made from this solution ending at 10 cells/µL. Two microliters of each dilution sample was then spotted on YPD plates at room temperature, 30°C, and 37°C. Growth was assessed after several days.

RESULTS

Regulatable *MTW1*

As Mis12p/Mtw1p had been implicated as essential for chromosome division and viability in other fungal species, previous studies on this and other kinetochore proteins have used conditional mutant phenotypes (Goshima et al., 1999; Goshima and Yanagida, 2000; Roy and Sanyal, 2011). For these reasons we sought to create strains bearing conditional phenotypes for *CnMTW1*. Two approaches were used to achieve this goal: an amino acid substitution resulting in a temperature-sensitive mutant phenotype and a promoter-swap construct that replaces the native *CnMTW1* promoter with the regulatable *CTR4* promoter.

CnMtw1p Shares Evolutionarily Conserved Core Domain

Protein sequence alignments performed with Mtw1/Mis12 homologs from various fungal species indicates that the gene being studied is highly similar to the previously studied homologs. The sequence of CnMtw1p, for instance, is 17.9% identical to that of SpMis12p (see Table 4), the protein homolog originally described as having this particular role in the kinetochore. As described in a previous study (Roy et al., 2011), two regions of high homology exist near the amino terminus of the Mtw1p homologues with the first one stretching from the 58th amino acid residue of CnMtw1p to the 90th residue and the second one ranging from the 105th residue to the 137th. This second area is the most highly conserved region of the protein, with several residues showing no divergence across most of the sequenced fungal proteomes. These two regions are shown in this alignment to be present in the *Cryptococcal* Mtw1p sequence (Figure 1 below).

One of the residues found in the second region of homology, G109, is the analogous locus chosen in previous studies to make temperature-sensitive mutants of this protein through the substitution of this nonpolar residue with the negatively charged glutamic acid. The high sequence similarity between ScMtw1p and CnMtw1p along with the presence of the highly conserved amino-terminal segments of CnMtw1p strongly suggest that this is indeed the structural homologue in *C. neoformans*.

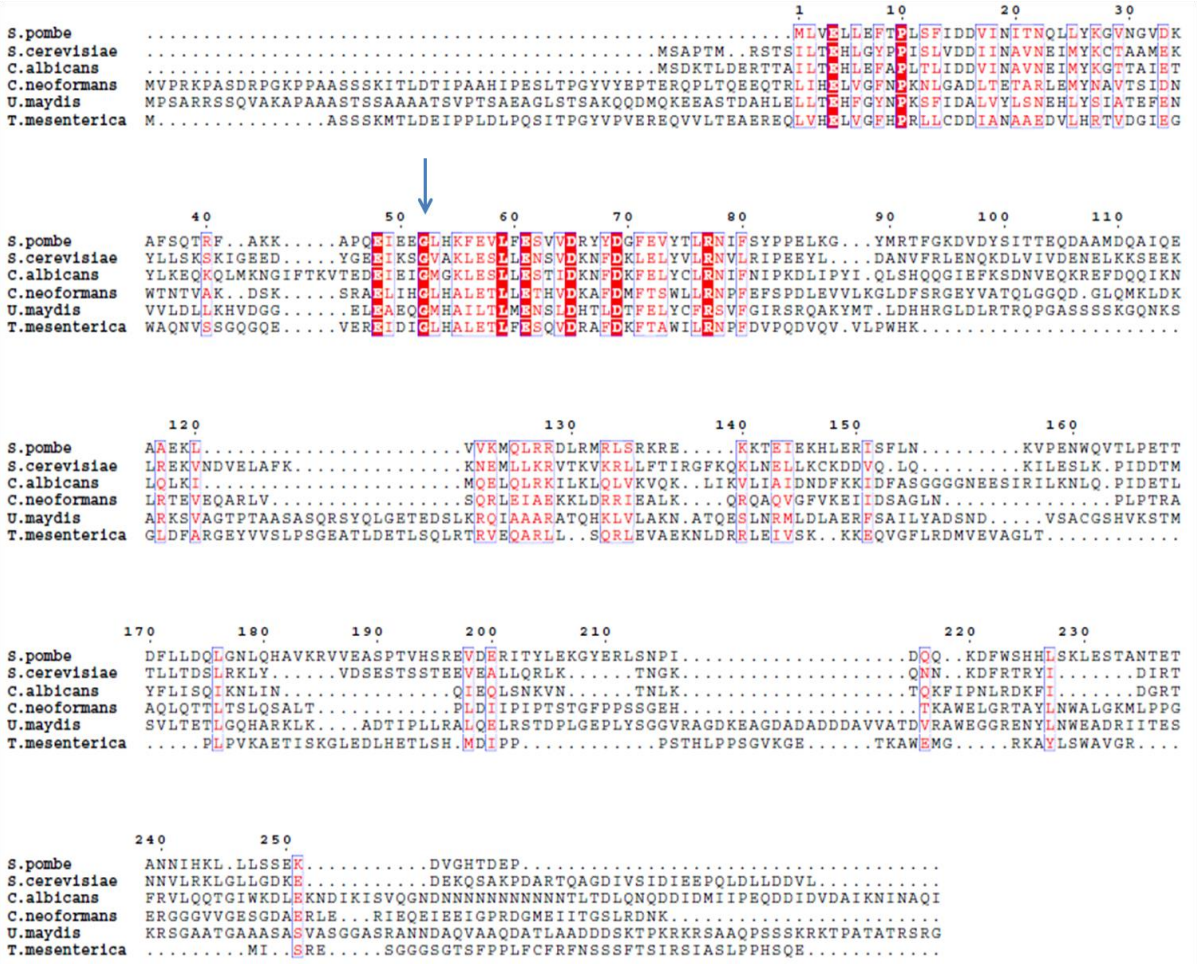

Figure 1. Amino acid sequence alignment of CnMtw1 with fungal homologs. Identical sequences are highlighted in dark red, similar residues are colored light red. The conserved glycine residue targeted for mutation is denoted by the blue arrow.

$\underline{P_{CTR4}}$ Promoter Swap Overlap PCR

Creating a genetic construct in which the native promoter is replaced with an exogenous one via overlap PCR requires numerous PCRs to create template to perform the final overlap reaction. The scheme is diagrammed below in Figure 2. For the *MTW1* promoter swap, two initial PCRs were performed using a strain in which *MTW1* was tagged with *mCherry* and NEO^R. One PCR was performed to amplify the 5' UTR region of the *MTW1* gene, while a second reaction amplified the *MTW1* gene tagged with *mCherry*, the neomycin (NEO^R) selectable marker, and approximately a kilobase of *MTW1* 3' UTR from the parent strain. Both of these PCR fragments contained small sequences from the *CTR4* promoter for use in the overlap PCR. A third PCR was performed off of P_{CTR4} plasmids created by Ory et al. (2004) to generate template that included the entire *CTR4* promoter in addition to *MTW1* 5' UTR sequence on its 5' side and the initial 15 bp of *MTW1* coding sequence on its 3' side. The product of this third reaction has terminal sequences homologous to one of the ends of each of the first two products. These bits of homologous, overlapping sequence allow the templates to be stitched together during the final overlap PCR.

The products of these reactions are shown below in Figure 3. The second lane displays the 5' UTR amplicon at the expected 732 bp, with the 3' *MTW1-mCh-*NEO^R amplicon showing in the third lane at 5.3 kb. The two P_{CTR4} promoter construct amplicons are shown in the fourth and fifth lanes. Both reactions were successful with bands at 450 bp and 700 bp, respectively; however, bands of both sizes are present in the fifth lane. This indicates that the reaction that generated the correct construct with both promoter elements also yielded a product with just one element. To avoid the

complication of generating both types of overlap fragments in the same PCR reaction, the desired P_{CTR4} fragment was gel purified from the fifth lane before use as template in the final PCR. The last two lanes show the product of the overlap PCRs performed with the P_{CTR4} and P_{CTR4}-*2* constructs, respectively. These lanes show bands in the 6.5 kb region, indicating successful construction of the overlap construct. The band in the last lane appears to migrate a little slower than that in the lane before it, indicating a slightly larger size as would be expected due to the extra promoter element. These results indicate that the desired P_{CTR4} promoter constructs were successfully created by the final overlap reaction.

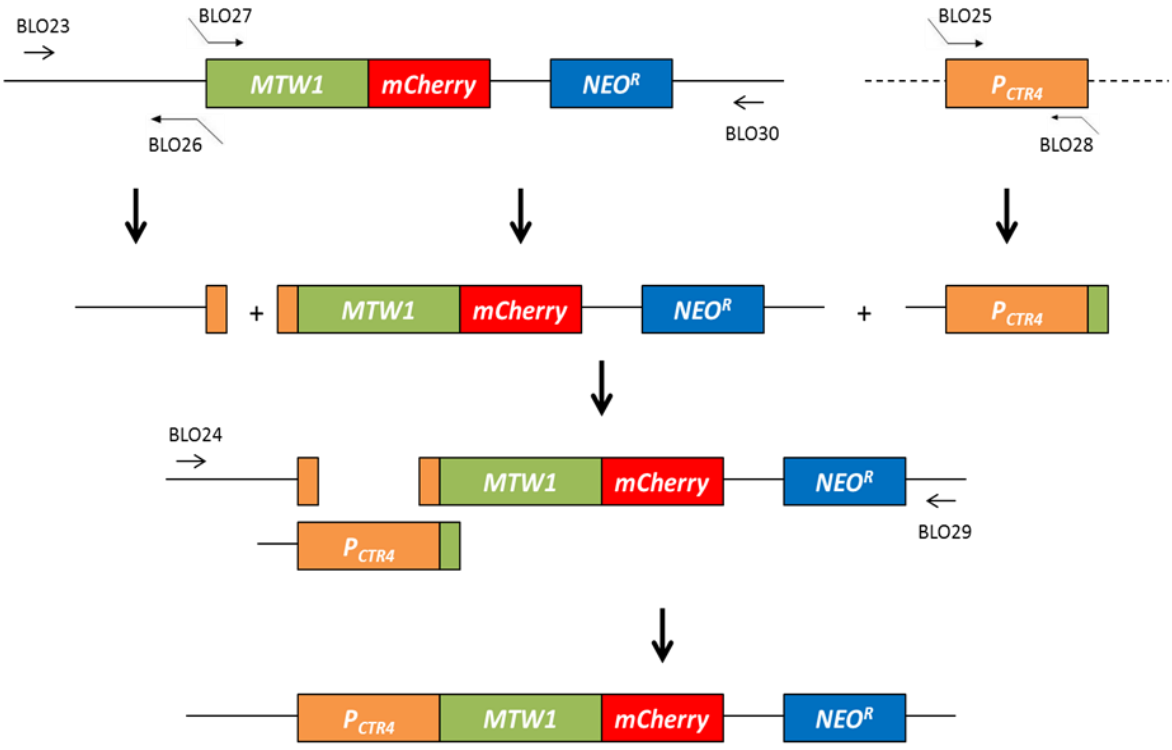

Figure 2. Diagrammatic scheme for P_{CTR4} promoter swap overlap PCR. Shown at the top are the two sources of DNA for this construct: the *mCherry*/*NEO*^{R} tagged *MTW1* construct and the P_{CTR4} promoter construct as found in the P_{CTR4} plasmid (backbone denoted by dashed lines). Forward and reverse primers used in each PCR are shown above and below, respectively, for each template. Primers are labeled with their names. Kinked portions of overlap primers represent non-homologous sequence.

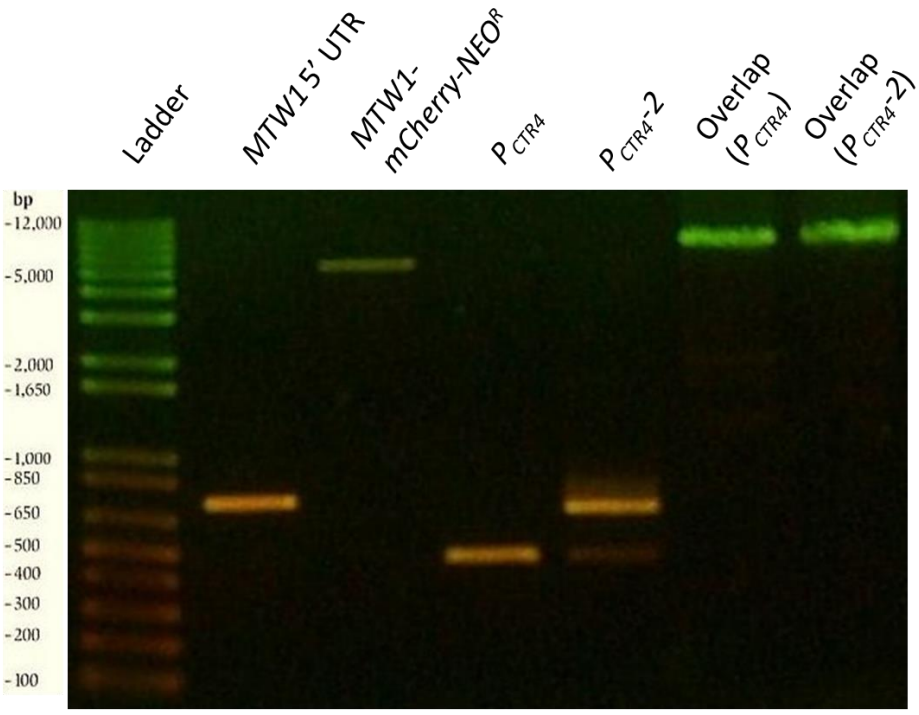

Figure 3. Agarose gel electrophoresis of P_{CTR4} promoter swap overlap fragments. An Invitrogen 1 kb plus ladder was used in the first lane. The *MTW1* 5' UTR PCR product is shown in the second lane while the third lane shows the 3' *MTW1-mCherry-NEO*^{R} construct PCR product. The fourth and fifth lanes show the product of the P_{CTR4} and P_{CTR4}*-2* PCRs, respectively, while the last two lanes show the overlap products made from both PCRs.

Screening for Successful P_{CTR4}*-MTW1-mCherry* Transformants

Integration of the constructs generated through overlap PCR described above into the genome of *C. neoformans* was performed by biolistics. Insertion of the fragment at the correct site should place the *MTW1* gene under the control of the copper-repressible promoter P_{CTR4}. In an attempt to identify P_{CTR4}*-MTW1* transformant strains in which the promoter sequences were properly exchanged, colonies that arose from the biolistic plates were streaked onto plates containing the copper chelator BCS and the drug G418 to select for putative transformants containing the neomycin resistance gene. These strains were

then replica plated on BCS or $CuSO_4$-containing media (Figure 4) to screen for cells exhibiting growth defects in response to repression of the regulatable P_{CTR4} promoter in the presence of copper sulfate. However, despite screening more than 200 transformants, no isolates displayed any significant difference in growth between the two media. One transformant strain, named P_{CTR4}-*MTW1*, was isolated that showed the conditional phenotype initially but lost it upon subsequent passages. This may indicate either that no transformant strains were isolated that contained the construct successfully integrated into the correct locus or that downregulation of *MTW1* expression has no evident effect on growth on solid media.

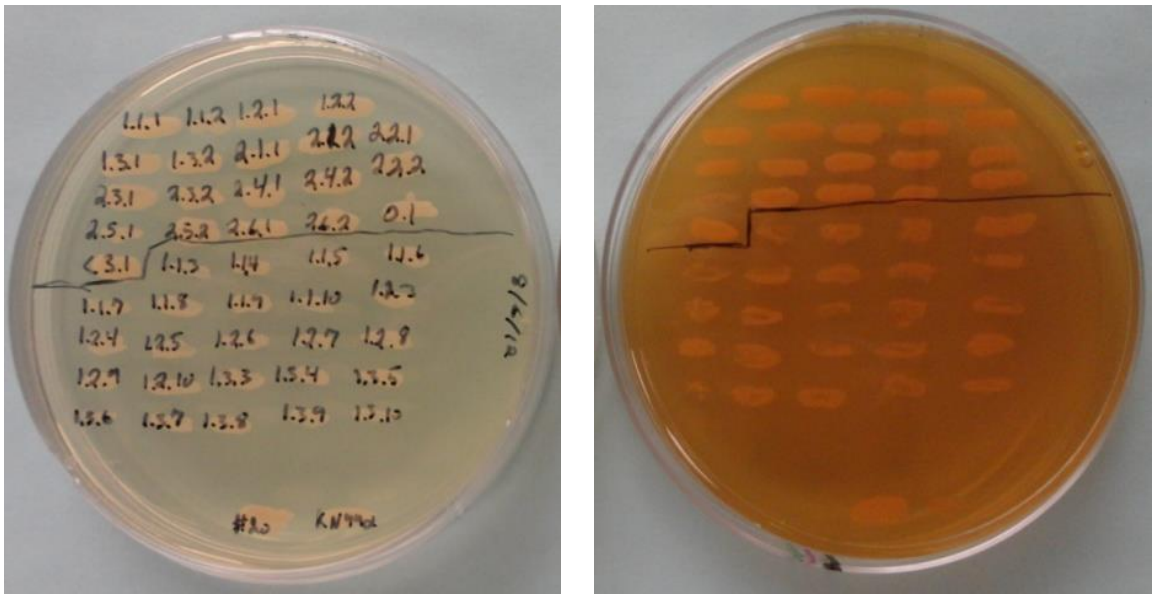

Figure 4. Results of P_{CTR4} transformant plating. Putative transformant strains are shown after 4 days growth on 25 µM $CuSO_4$ (left) and 200 µM BCS (right). IBCN#20 (*MTW1-mCherry NEO*^{R}) and IBCN#2 (KN99α wt) were streaked at the bottom of each plate as controls for growth on these media.

Generation of a temperature-sensitive *MTW1* mutant

In order to create the genetic construct required to induce the temperature-sensitive conditional mutation in *MTW1*, primer pairs were designed such that regions upstream and downstream of the mutation site are amplified and made to include an overlapping sequence containing the site of interest and the desired mutation. This amount of overlap allows these amplicons to be fused upon PCR using primers far upstream and downstream of the mutation site. The final product of the overlap PCR process is a genetic construct that contains the mutated gene of interest and around one kilobase of flanking sequence on either side. For the purposes of identifying successful transformants a selective marker, such as the neomycin (G418) resistance gene, is included in the final product while the protein encoded by the gene of interest may be tagged with a fluorescent protein immediately downstream as a means of visual detection. For this experiment a strain of *C. neoformans* containing an *mCherry*-tagged copy of *MTW1* with a neomycin resistance gene downstream of *MTW1* was used as a source of genetic material.

Creating a construct for a putative temperature sensitive *MTW1*

A site-specific mutant construct was created using a similar overlap PCR method as that of the promoter swap. Creating a mutant construct was simpler, however, in that it only required the generation of two overlap templates with which to perform the final PCR as opposed to the three-piece overlap strategy used for the promoter swap overlap. The scheme followed is shown below in Figure 5. The first PCR was run to create a 5' UTR amplicon containing 797 bp of native promoter sequence immediately upstream of

the *MTW1* start codon up through the region of interest, including 483 bp of genomic sequence and the two mutant base pairs to be incorporated in the final product. A second reaction was performed creating a 4820 bp template that included 706 bp of *MTW1* 3' UTR along with the *mCh-NEO*^{R} cassette from the parent strain and 852 bp of *MTW1* including the region of interest and the mutant base pairs. These two products shared 35 bp of overlapping sequence and were used as the templates in the final overlap PCR.

The results of the initial PCRs performed to generate templates for the final overlap are show in Figure 6, where the products have been separated on an 0.8% agarose gel. A band is present around 1280 bp in the upstream PCR lane, corresponding to the predicted size of this amplicon. In the downstream lane a band is present at ~4.8 kb, as predicted for the construct fragment containing the neomycin resistance gene, *mCherry*, and most of *MTW1*. In lane four of Figure 6, the purified overlap PCR product is seen as a band at ~6 kb. This is consistent with the size of the entire desired overlap construct (5975 bp), confirming its successful generation. However, this is also the size of the native, non-mutant construct containing the *mCherry-NEO*^{R} construct that may be generated as a side product of these reactions.

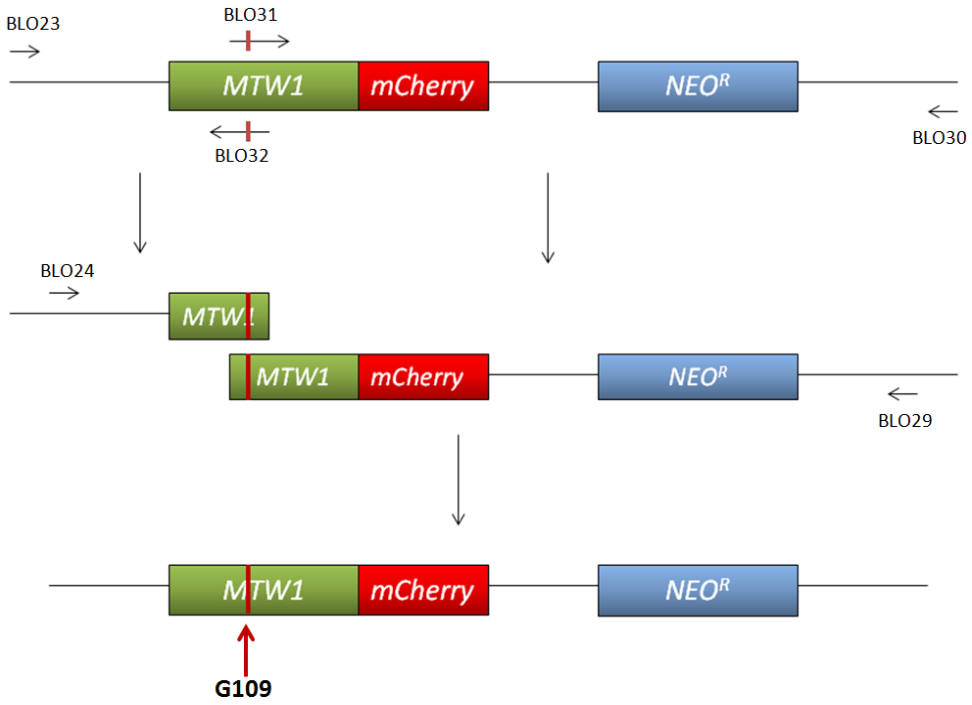

Figure 5. Generation of the temperature-sensitive *MTW1* mutant construct. Shown at the top is the configuration of genetic components for the region of interest as found in the *MTW1-mCh-Neo* #20 strain. Primer designations for each reaction are shown above and below each construct for the forward and reverse primers, respectively. The mutation site, G109, is show by the red arrow. The red bars within BLO31, BLO32, and amplified regions of *MTW1* represent the site-specific mutation.

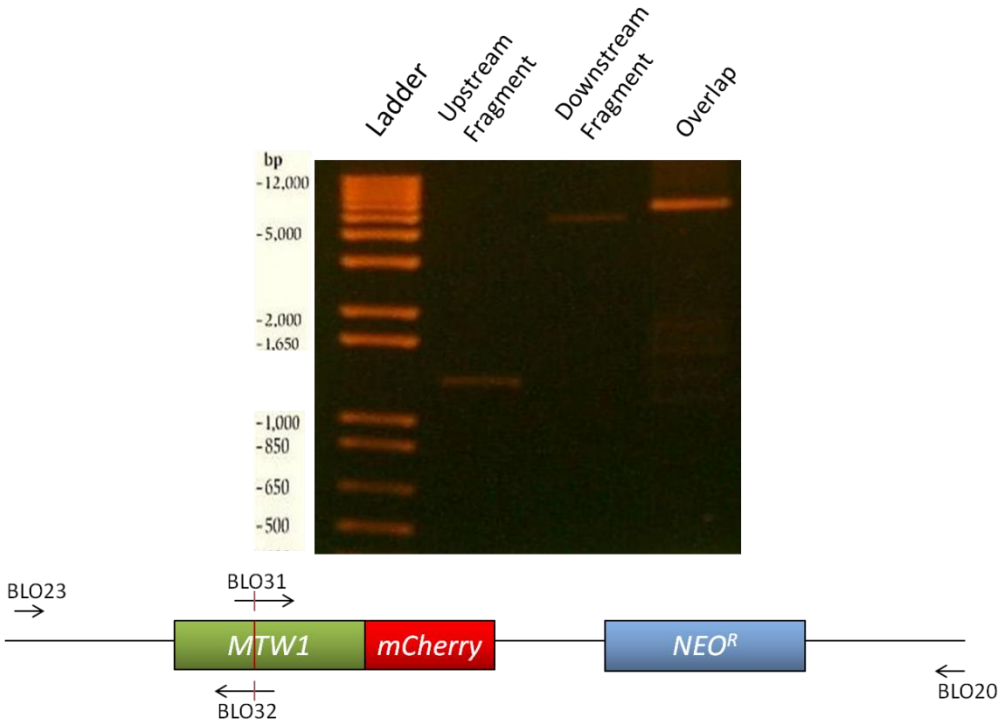

Figure 6. Agarose gel electrophoresis of *ts-MTW1* overlap fragments. The first lane contains the Invitrogen 1 kb plus ladder. The second lane contains the product of the 5' upstream PCR while the third lane contains that of the 3' downstream PCR. The final lane shows the product of the overlap PCR performed with the products in two prior lanes serving as templates.

Identification of Potential Mutants

In order to identify transformant strains that might contain the desired mutagenic sequence, colonies were sampled from the biolistics recovery plate and streaked for singles on YPD-Neo plates and incubated at room temperature (23°C). The resultant colonies were streaked on YPD plates at 23°C, 30°C, and 37°C to determine whether any of the colonies were unable to survive at the higher temperatures. The wild type KN99α strain was also streaked on these plates as a control. Strains that appeared to either not grow or grow less quickly at 37°C as compared to the lower temperatures were selected for further examination and molecular diagnostics. The initial growth assays on plates

provided a number of potential mutant strains that displayed inhibited growth at the restrictive temperature. These strains were then tested on YPD-Neo at both 23°C and 37°C two more times to confirm the temperature sensitive phenotype. An example of such growth inhibition is shown below in Figure 7, where several strains capable of growth at room temperature (left) fail to grow at body temperature (right). After three rounds of growth assays on solid media, seven strains were selected for molecular diagnostics: 1.21, 1.25, 1.28, 1.31, 2.16, 3.18, 3.25.

It is possible that the temperature sensitive phenotype is masked when cells are grown in solid media. This may be due to the possibility of cells reaching a maximum density that is less than that when cells are grown in liquid media.

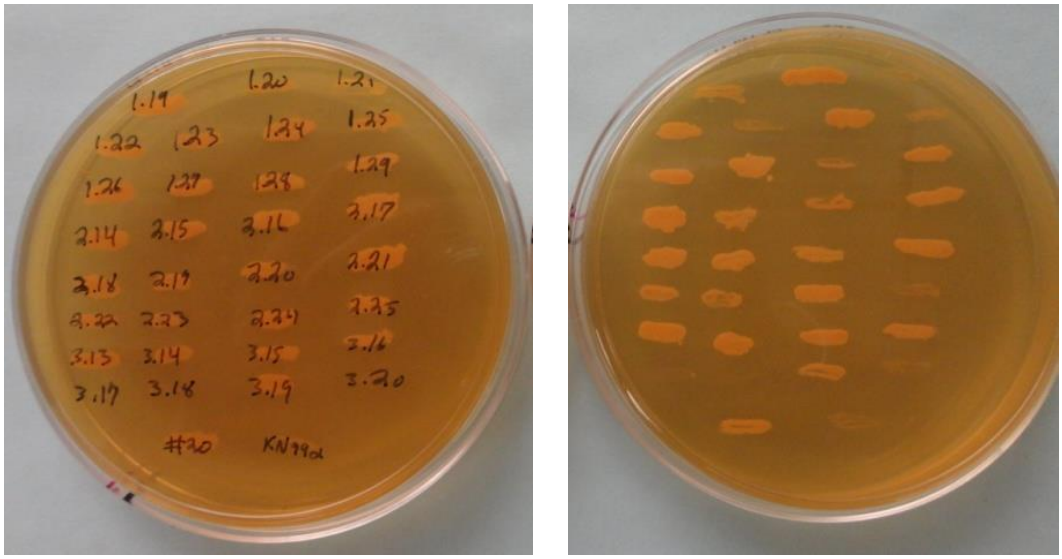

Figure 7. Results of initial temperature assay. Strains were streaked on YPD/Neo and grown at the listed temperatures for three days. IBCN#20 (*MTW1-mCherry NEO*^{R}) and IBCN#2 (KN99α, wt) were streaked at the bottom of each plate as controls for this medium.

Insert Diagnostics

Two of the putative ts strains were shown to have integrated the complete construct. As seen in Figure 8, strains ts 1.28 and 2.16, denoted by red asterisks, produced a band at ~6 kb. This is the same size as the band produced when the same PCR was performed on the positive control parental strain *MTW1-mCh* #20 (lane four). The presence of the larger band as the PCR product for these two strains indicates that the entire construct was integrated into the *Cryptococcal* genome. However, this does not necessarily indicate that the construct has integrated into the genome in the correct position and orientation. For this reason, further PCRs were designed to determine whether the native sequence was correctly replaced with the mutant construct.

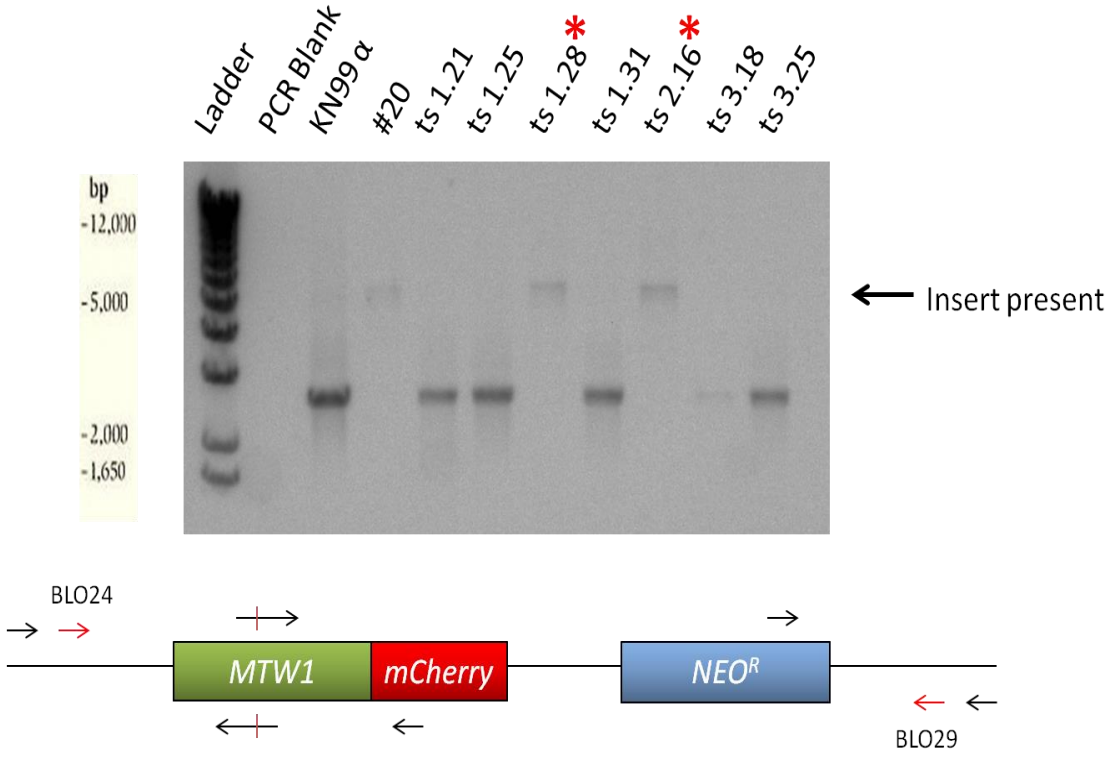

Figure 8. Whole construct confirmation. PCR products showing the presence of either the wild type or construct-containing sequences. Primers used are indicated in red at the bottom. Lanes showing the construct of interest are denoted with an asterisk. The size of the insert is indicated by the arrow at the right.

The next round of diagnostic PCRs sought to demonstrate the presence or absence of the mutant construct at the correct site and orientation in the genome. One PCR was designed to check the 5' end of the construct, using a forward primer in the *MTW1* 5'UTR upstream of where the construct should integrate and a reverse primer homologous to the *mCherry* sequence. These diagnostics were performed on genomic DNA isolated from the P_{CTR4}-*MTW1* strain (Figure 9a) and the ts-MTW1 transformants (Figure 9b) along with positive and negative controls. For the ts strains, if the construct has been integrated correctly, a product should be made that is 2266 bp large as shown by the positive control *MTW1-mCh* #20 in lane four whereas the product for the P_{CTR4}-*MTW1* transformant should produce a band of 2.5 kb. If the *mCherry* sequence is not present in the correct locus and orientation, then no product should be made as a result of this PCR. This is exemplified by the absence of a band produced from the KN99α wild type strain. As before for the ts strains, only strains ts 1.28 and ts 2.16 displayed bands of the correct size at approximately 2.3 kb in the sixth and seventh lanes. The second PCR was designed to see if the 3' end has correctly integrated by using a forward primer within the NEO^R cassette and a reverse primer in the *MTW1* 3' UTR downstream of where the construct should integrate. As before, a product should only be made if the construct has successfully replaced the native sequence. In agreement with prior PCRs, bands were seen only for the positive control (lane 13) and strains ts 1.28 and 2.16 (lanes 15 and 16). Taken together, the results of these three diagnostic PCRs on putative ts stains confirm that the native *MTW1* sequence was replaced with the *MTW1-mCherry* NEO^R construct in two strains: ts 1.28 and ts 2.16. In addition, the P_{CTR4}-*MTW1* strain displayed a band of the correct size for both the 5' and 3' integration regions (Figure 9a).

This indicates that the *CTR4* promoter sequence was integrated into the correct cryptococcal locus and that we have successfully generated a strain with a conditional promoter upstream of the *MTW1* coding sequence.

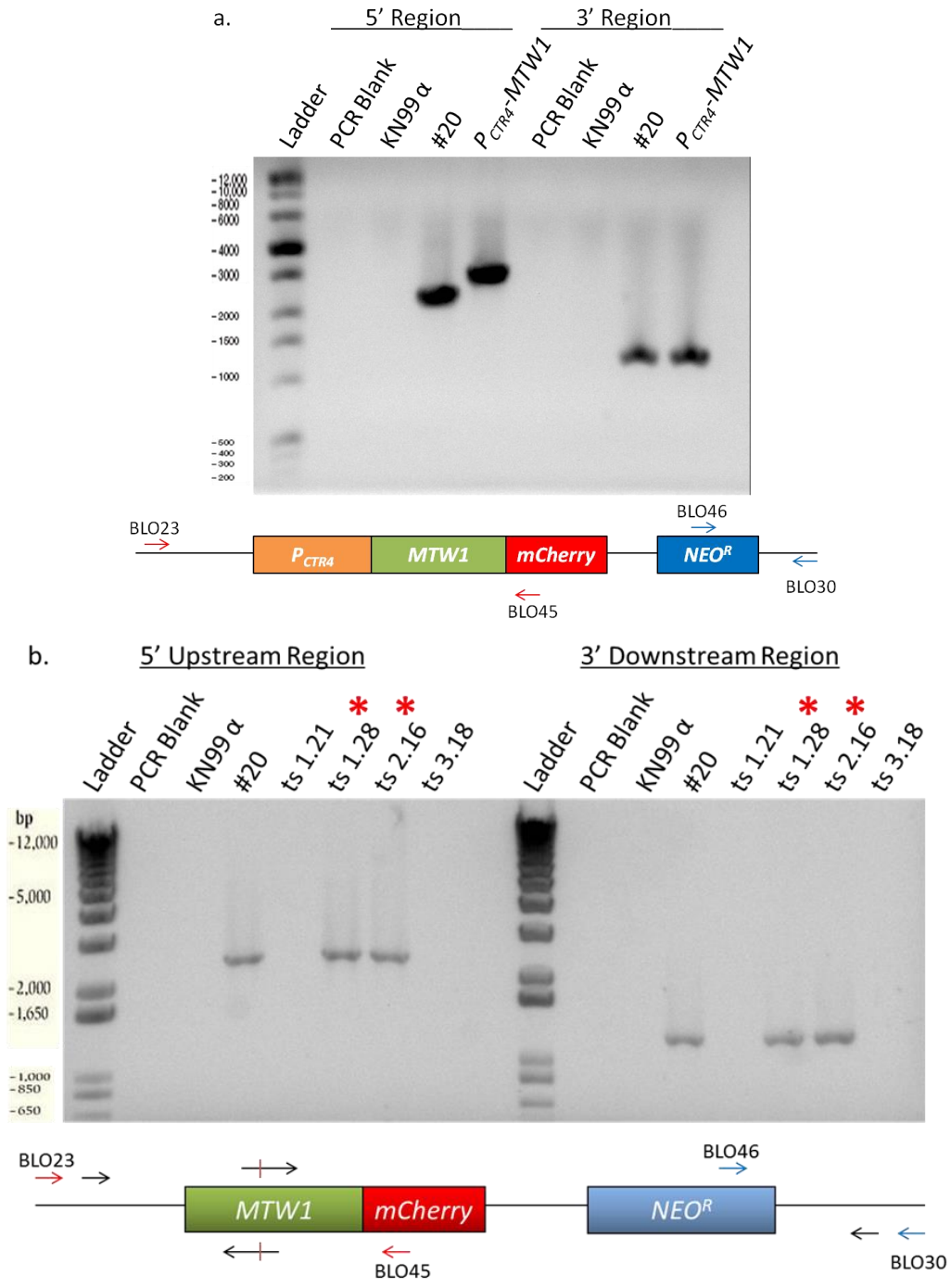

Figure 9. Upstream and downstream orientation confirmations. a. *P_{CTR4}-MTW1* insert diagnostic PCRs. b. ts-MTW1 insert diagnostic PCRs. On the left of each gel are PCR products from the left side of the construct from the 5' out primer to the mCherry antisense primer (primers in red at bottom). On the right side of each gel are PCR products from the right side of the construct from the NEO^R sense primer to the 3' out primer (primers in blue at bottom). Lanes that contain the correct product are marked with an asterisk.

Strains that had shown correct integration of the *MTW1-mCherry NEO^R* construct were selected to have genomic DNA from the region surrounding the mutational site of interest, including 1.2 kb upstream and about 1 kb downstream, sequenced to determine whether any contained the intended mutation. Control strain KN99α was used to confirm the wild type sequence while IBCN#20 (*MTW1-mCh NEO^R*) was sequenced to confirm the wild type sequence of the parental DNA used to make the mutagenic constructs. As shown below in Table 3, these two stains did contain the wild type sequence. Strains IBCN#21 and IBCN#22 describe two mutants created prior to this experiment that were designed to include mutations at the desired site. These strains were included to determine whether they did in fact code for mutants. As shown in Table 3, both of these strains contained the sequence "AT" at the mutational site of interest. This shows a transition mutation from guanine to adenine within the coding sequence. This mutant sequence should result in replacing the highly conserved non-polar glycine residue with the polar aspartic acid residue. Sequencing results from transformants produced during the course of this experiment are shown at the bottom of Table 3. Only one of the three strains chosen for sequencing contained a mutant sequence. Strain ts 1.28 contained the desired "GT" to "AA" mutation, resulting in the glycine to glutamic acid mutation used for previous studies while strains ts 2.16 and ts 3.18 contained only the wild type sequence.

The results of this sequencing indicate that at least one biolistic transformant contained the mutant sequence designed in this experiment to replace the conserved glycine residue with glutamic acid. Sequencing has also shown that the strains made prior to this experiment also contain a sequence coding for a glycine mutant. Despite the

fact that this mutant codes for aspartic acid instead of glutamic acid, the mutation chosen in previous studies, the end results in terms of protein thermostability may be the same. This is due to the structural homology between aspartic and glutamic acids: both are amino acids with acidic side chain. The only difference is that aspartic acid has one less hydrocarbon in its side chain. This implies that for the purpose of testing temperature sensitive *MTW1* mutants the aspartic acid mutants may be functionally homologous to the glutamic acid mutants and should therefore be included in further experiments.

Table 3. Transformant *MTW1* sequences. Shown in the table below are the sequences obtained from a number of biolistically transformed strains from two independent sequencing reactions (sense and antisense strands). KN99α represents the untransformed wild type while *MTW1-mCh* is the strain from which the mutant constructs were derived. Nucleotides in red indicate the two target nucleotides to be mutated. The final column describes the amino acid produced at the mutation site, with WT representing the native glycine residue.

Strain	From the Forward Primer (BLO34)	From the Reverse Primer (BLO49)	Mutation
KN99α	GATTTGTCATTCTAGG**GT**CTGCATGCTTTAGAAAC	GTTTCTAAAGCATGCAG**AC**CCTAGAATGACAAATC	WT
***MTW1*-mCh**	GATTTGTCATTCTAGG**GT**CTGCATGCTTTAGAAAC	GTTTCTAAAGCATGCAG**AC**CCTAGAATGACAAATC	WT
#21	GATTTGTCATTCTAGG**AT**CTGCATGCTTTAGAAAC	GTTTCTAAAGCATGCAG**AT**CCTAGAATGACAAATC	G → D
#22	GATTTGTCATTCTAGG**AT**CTGCATGCTTTAGAAAC	GTTTCTAAAGCATGCAG**AT**CCTAGAATGACAAATC	G → D
1.28	GATTTGTCATTCTAGG**AA**CTGCATGCTTTAGAAAC	GTTTCTAAAGCATGCAG**TT**CCTAGAATGACAAATC	G → E
2.16	GATTTGTCATTCTAGG**GT**CTGCATGCTTTAGAAAC	GTTTCTAAAGCATGCAG**AC**CCTAGAATGACAAATC	WT
3.18	GATTTGTCATTCTAGG**GT**CTGCATGCTTTAGAAAC	GTTTCTAAAGCATGCAG**AC**CCTAGAATGACAAATC	WT

Characterizing the ts-*mtw1* Transformants

Once it had been established that a mutant strain had been created with the desired glycine to glutamic acid mutation and that two strains created previously had a similar aspartic acid substitution at the same locus, several assays were performed to assess the effect of these mutations on growth and cell cycle progression. Strains found to contain mutant sequences were streaked on YPD at 23°C, 30°C, and 37°C (Figure 10). After 2 days growth, the KN99α wt strain grew equally well at 30°C and 37°C, with less growth seen at 23°C. This result was also obtained with IBCN#20, IBCN#21 (G109D), and G109E. IBCN#22 was exceptional in that it showed significantly less growth at 37°C as compared to 30°C. The plating results of spot assays performed at three different temperatures after 3 days, shown below in Figure 11, are largely in agreement with the streaking assay. KN99α grew robustly at 30°C, with less growth at 37°C and even less at 23°C. This pattern was seen for both IBCN#20 and IBCN#21 (G109D). IBCN#22 grew less robustly than the other strains at all temperatures; however, this strain only grew marginally at the restrictive temperature with growth spots that were barely visible.

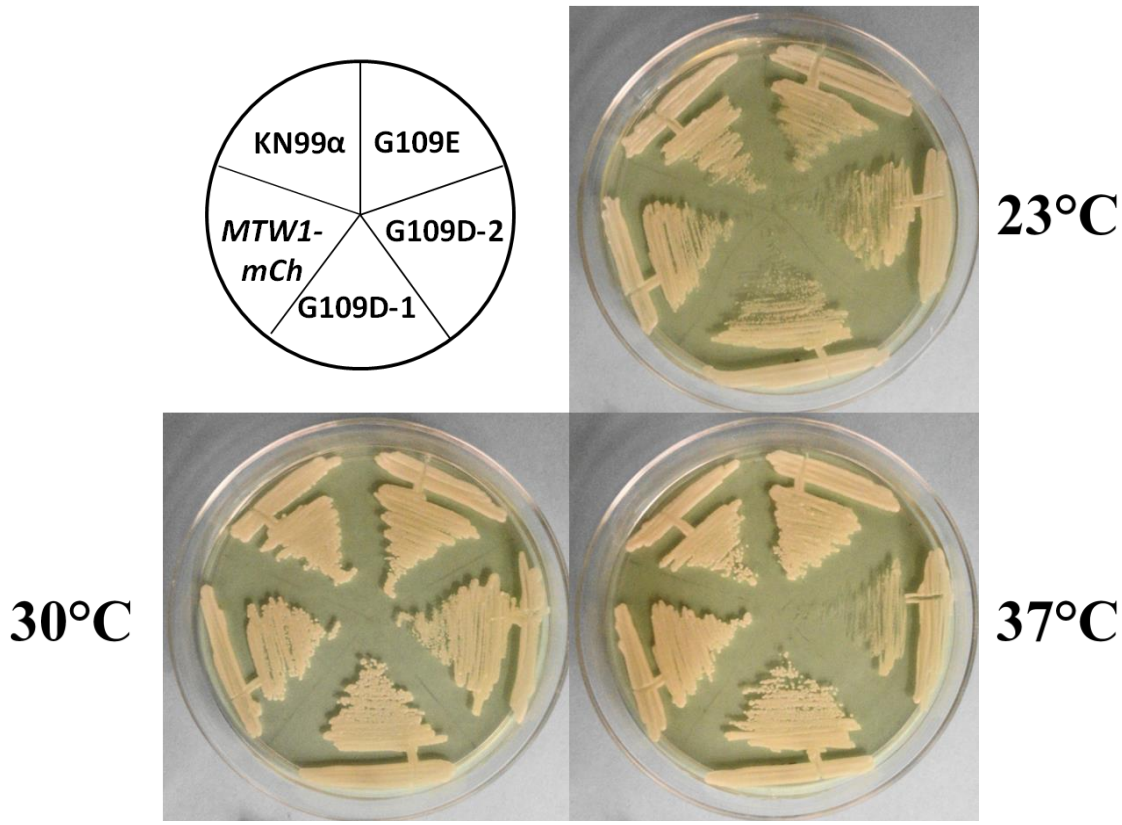

Figure 10. Growth of mutant strains on solid media. Strains were streaked on YPD media and incubated at the indicated temperatures for two days.

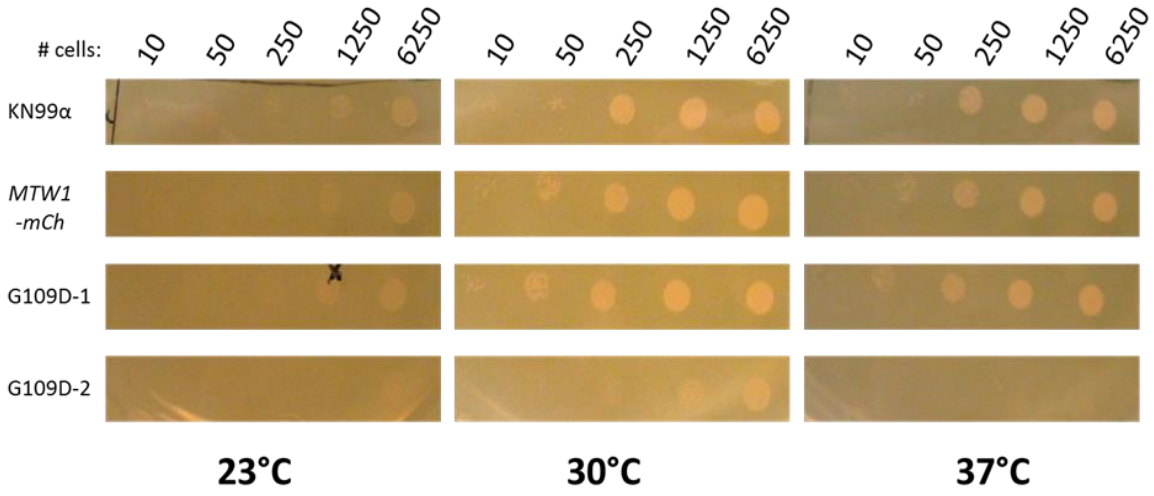

Figure 11. Temperature-sensitive (ts) spot assay. Shown above are the results of spot assays performed with putative ts cells. Spots were made in triplicate with one plate incubated at 23°C, one at 30°C, and one at 37°C.

The next step to analyzing the growth of these mutant strains under restrictive vs. permissive conditions was to assess their rates of growth in liquid media and the budding state distribution of populations at different time points. As seen in the growth analysis in Figure 12, at 30°C (left), the two mutant strains grew equally as well as the wild type and all three strains grew well. This contrasts with growth in general at 37°C, as evidenced by the lower rates of growth for all three strains. Despite this general effect, the two mutant strains displayed less growth at the restrictive temperature. Growth inhibition at 37°C appeared to be reversible as shifting cells from 37°C to 30°C resulted in normal growth rates for all strains. Samples were taken from this growth assay to perform phenotypic assessment.

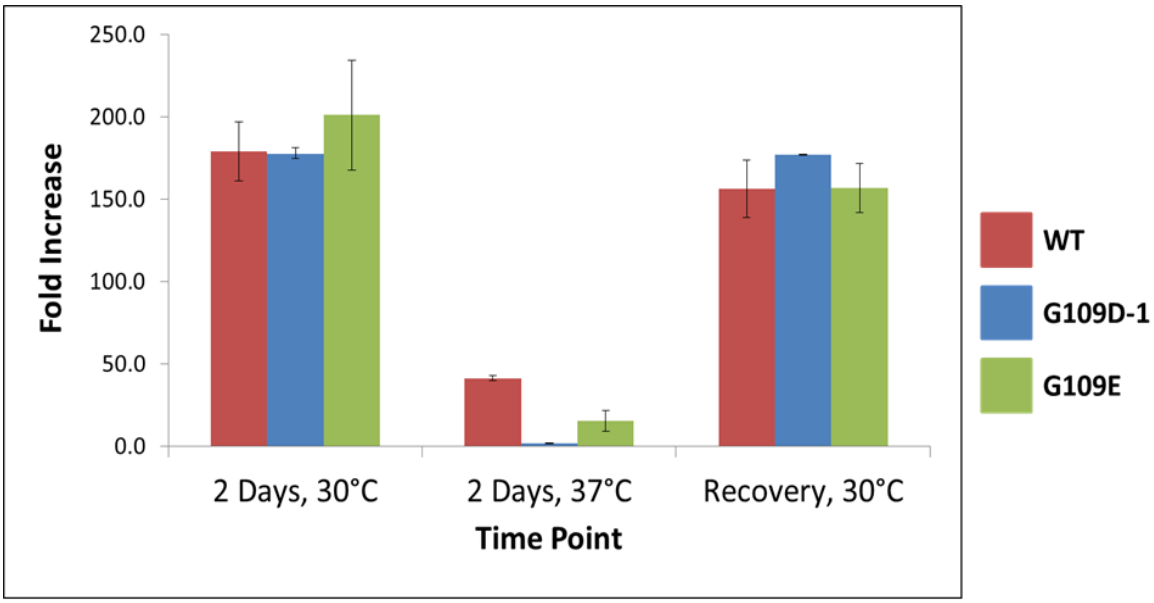

Figure 12. Growth analysis for ts strains at 30°C and 37°C. Bars represent one standard error. The cells grown at 37°C were shifted to 30° after two days for a recovery period.

Phenotypic Assessment

The budding state distributions of these samples are shown in Figure 13 below for the two mutant strains and the wild type when cultured at 30°C and 37°C. After two days growth at 30°C, all three strains have reached stationary phase with approximately 90% of each population composed of unbudded cells. There is no significant difference in the budding state distributions in the mutants compared to the wild type at this temperature. Differences are seen, however, at 37°C, wherein all strains show increases in budding. In the wild type KN99α strain, the ratios of unbudded and small budded cells are significantly higher than those of large budded cells or mutants. This contrasts with the mutant strains, which show much higher frequencies of large budded and mutant cells. In strain G109E, large budded cells make up a significantly higher proportion of the population than small or medium budded cells. The situation is more extreme in G109D, in which the number of mutant cells equals that of unbudded cells and surpasses the other categories. In addition, G109D shows more large budded cells than small budded cells, the opposite situation of that found in the wild type population. Similar phenotypic characterization was performed on one strain (*P_{CTR4}-MTW1*) isolated from the *P_{CTR4}* construct transformations. No differences in growth on solid media or in liquid media were observed (data not shown); however, differences in the budding state distributions of populations under permissive and restrictive conditions were evident. As seen below in Figure 14, the wild type KN99α strain reached stationary phase after incubation for one day under each condition, with close to 90% of cells unbudded and a normal proportion of budding cells. The strain carrying the *P_{CTR4}-MTW1* construct displayed

normal budding phenotype in BCS media, while cells grown in $CuSO_4$ media showed gross aberrations in budding morphologies and distributions.

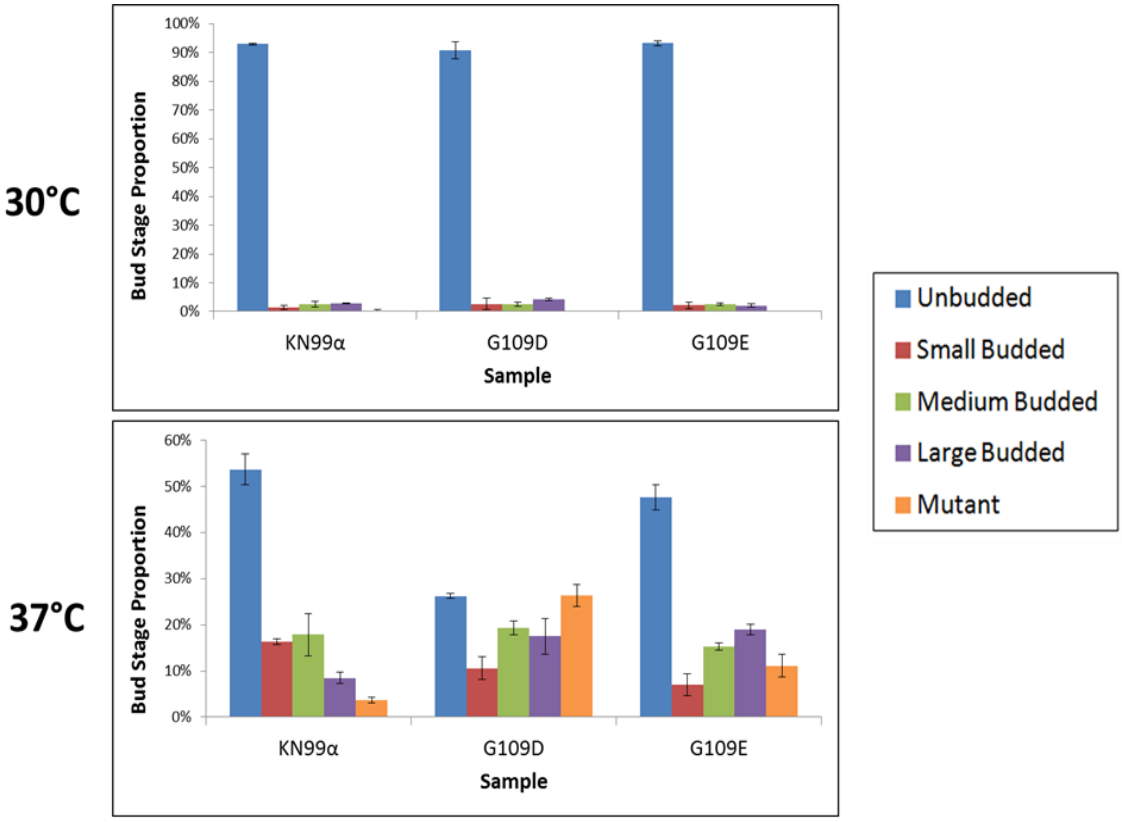

Figure 13. Temperature-sensitive bud counts. Budding states of different populations are shown for growth at 30°C and 37°C. Strains were cultured for two days in YPD. Error bars represent one standard error.

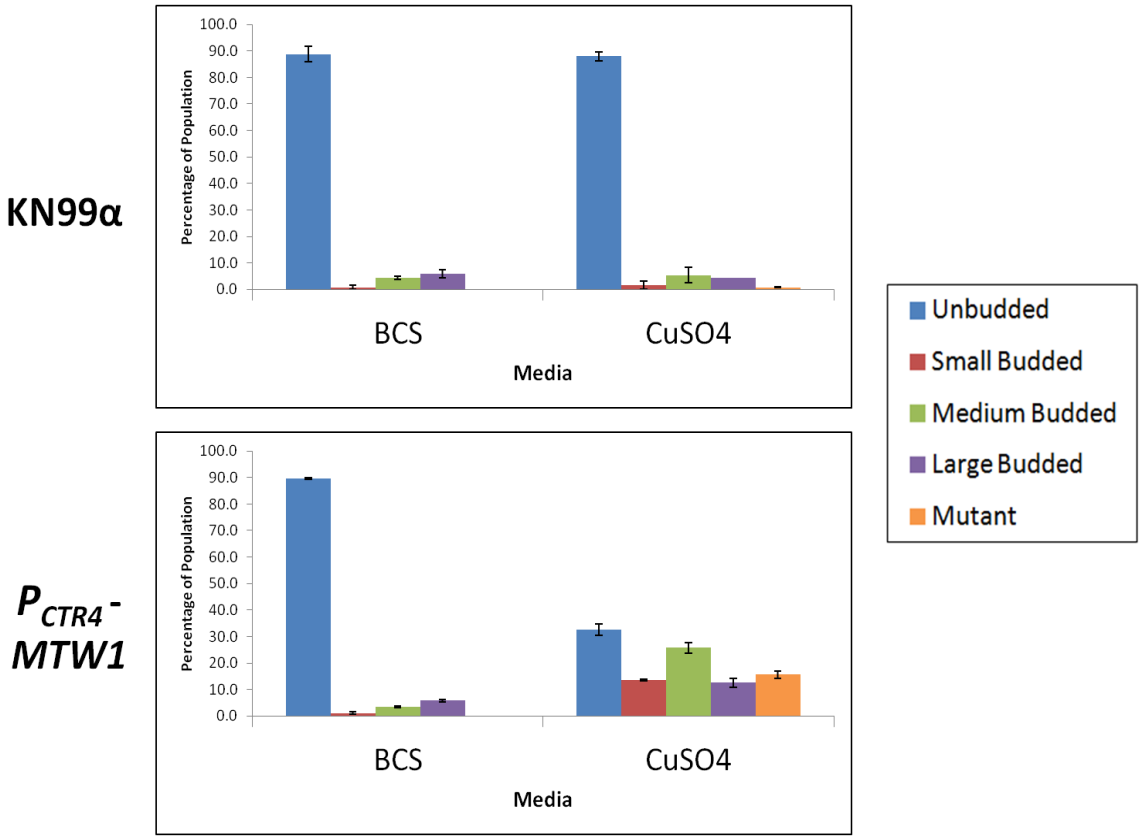

Figure 14. *P*$_{CTR4}$*–MTW1* bud counts. Results of bud count data are shown for KN99α (top) and *P*$_{CTR4}$*-MTW1* (bottom). Bars represent one standard error.

Microscopic analysis was performed on cells obtained from the above growth curve (Figure 15). DIC images of cells incubated at 30°C showed typical cell morphologies for the wild type strain and both mutants. DAPI staining revealed no abnormalities in nuclear DNA segregation in these cells. At 37°C, the wild type KN99α population was comprised mostly of cells with typical morphologies, with a low proportion displaying mutant morphologies. While most G109E cells appeared normal in phenotype at 37°C, budding mutants were found at a higher frequency compared to the wild type KN99 α strain. G109D displayed the most extreme and diverse mutant phenotypes at 37°C with some morphologies appearing as chains of budded but not detached cells and others as massive clumps of cells that were budding from the same

parent. DAPI staining of these cells revealed the presence of concentrated nuclear DNA in-between budding cells. In situations where one cell had budded incorrectly one time, DNA appeared to be stuck in the neck between parent and daughter cell.

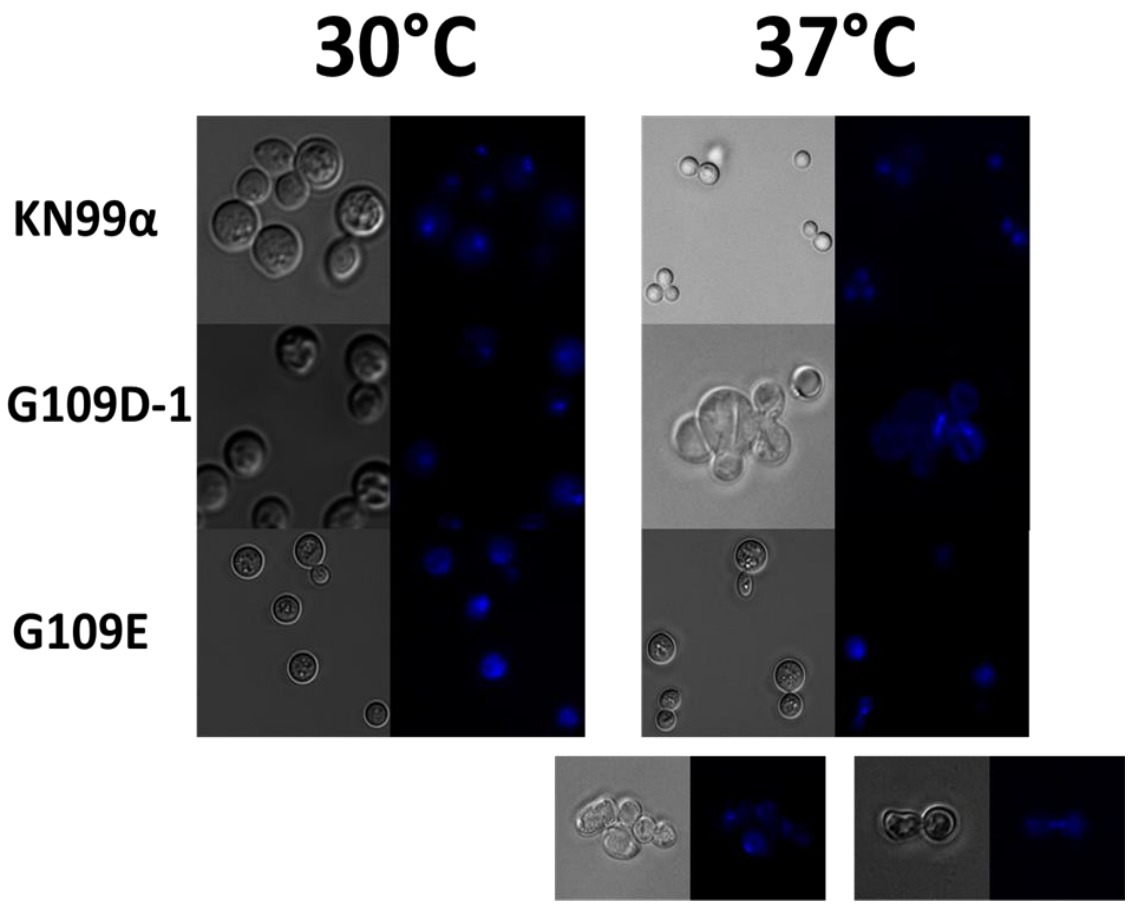

Figure 15. Morphological and nuclear characteristics of ts-*mtw1* mutants. Strains incubated at 30°C are shown on the left, those at 37°C on the right. DIC images are shown along with their corresponding DAPI images. Below the 37°C micrographs are shown additional images of mutant phenotypes obtained from the G109D-1 mutant.

RNAi of putative kinetochore proteins

The results obtained from the introduction of regulatable P_{CTR4}- and ts-*MTW1* constructs into the cryptococcal genome indicated that the role of *Mtw1p* may not be as essential to the viability of *C. neoformans* as its homologs have been shown to be for their species. As this result was not expected, RNA interference was pursued as a way to further probe the essentiality of *MTW1*. Additionally, other members of the *C. neoformans* kinetochore from the inner (*CSE4*, *MIF2*), middle (MIND complex), and outer (*DAD1*, *DAD2*) layers were selected for investigation through RNAi.

Amplification of Putative Kinetochore Homologs

In order to study the potential necessity for kinetochore proteins in *C. neoformans* the genes responsible for them had to first be identified. This was accomplished by searching for homologous amino acid sequences in the *C. neoformans* proteome using the genes originally described in *S. cerevisiae*. These DELTA-BLAST searches revealed the presence of one homolog each for the *S. cerevisiae* proteins *Cse4*, *Mif2*, *Mtw1*, *Nnf1*, *Nsl1*, *Dsn1*, *Dad1*, and *Dad2*. The loci revealed by these searches were analyzed for areas of high homology and used to amplify regions of genomic DNA coding for these proteins. The results of these PCRs are seen in the gels below (Figure 16). Each genomic insert was generated successfully, while amplifications from cDNA preparations made from genomic RNA preparations were typically unsuccessful.

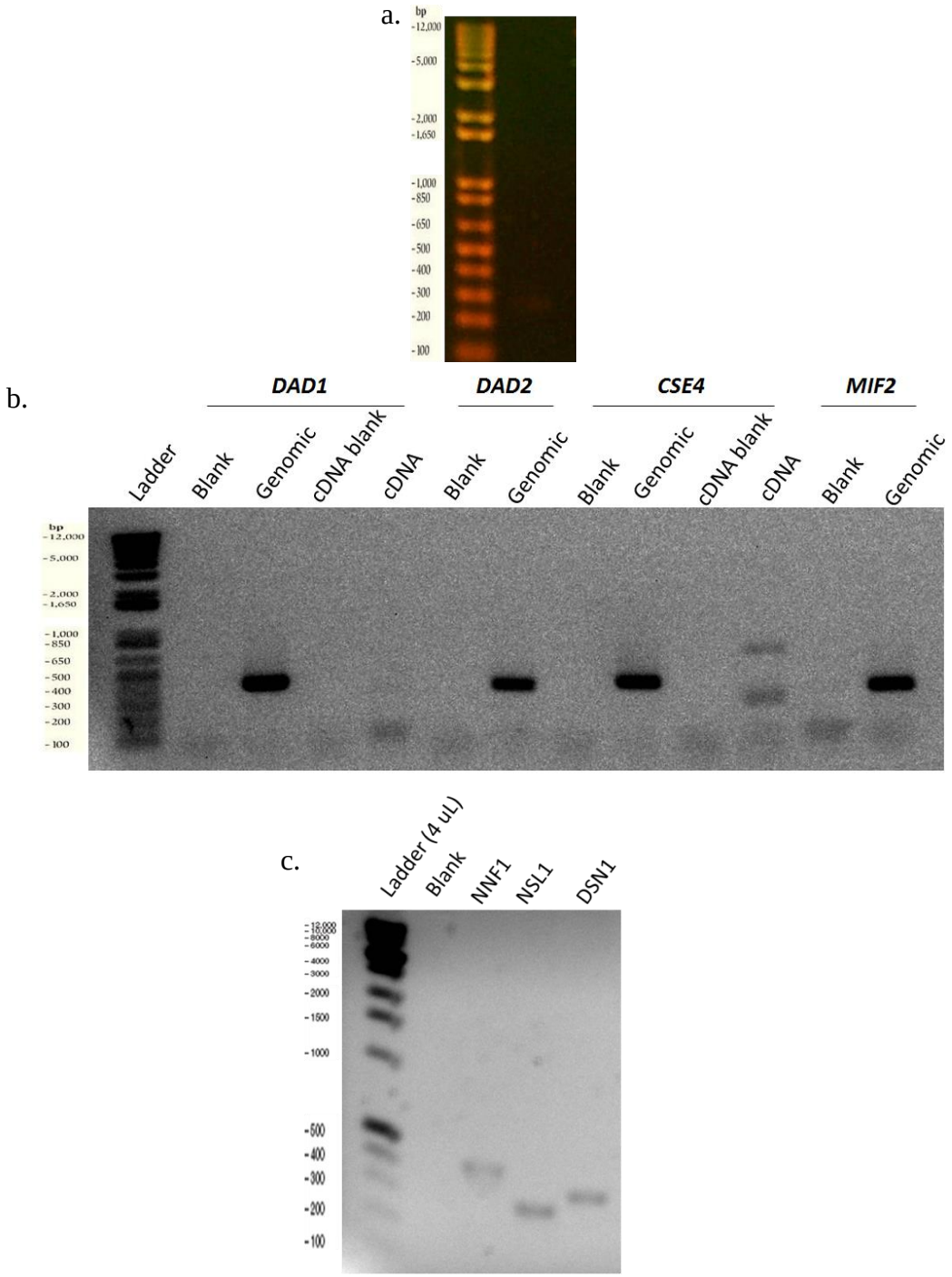

Figure 16. Generation of kinetochore RNAi inserts. The above gels show the results of PCRs to generate insert fragments for digestion and ligation into the RNAi vector. (a.) *MTW1* (second lane). (b.) The outer kinetochore genes *DAD1* and *DAD2* and the inner kinetochore genes *CSE4* and *MIF2*. (c.) MIND complex members *NNF1*, *NSL1*, and *DSN1*.

Construction of RNAi Plasmids and Transformation

After the desired sequences were ligated into the pIBB103 vector a restriction digest was restriction digests were performed on the RNAi plasmids as a diagnostic to demonstrate correct placement of the insert. PstI was used to digest pIBB103, p*CSE4*i, p*MIF2*i, p*DAD1*i, and p*DAD2*i. This enzyme targets three sites in the pIBB103 vector, two of which flank the RNAi cassette and one in the plasmid's backbone. Digestion with this enzyme should yield three fragments: one of 5.5 kb, one of 1.1 kb, and the third ranging from 2 to 2.5 kb. This last fragment should contain the gene insert and therefore will vary in size and act to confirm integration of the insert. The MIND complex RNAi plasmids were digested with different restriction enzymes to demonstrate their correct generation: p*MTW1*i plasmids were digested with BglII, p*NNF1*i plasmids with AgeI, p*NSL1*i plasmids with ScaI, and p*DSN1*i plasmids with SalI. These first two reactions should produce two bands if plasmid construction was successful whereas p*DSN1*i should be linearized by SalI if the construct integrated correctly. The results of these digests are shown below in Figure 17, where each plasmid displays the banding pattern that was expected, indicating successful plasmid creation.

Once the RNAi plasmids had been generated and shown to include the desired gene fragments the next step was to transform them into competent *C. neoformans* cells (Strain JEC21, IBCN#43) through electroporation, a method in which cells are exposed to an electric current for very short periods of time (on the order of milliseconds) that induces the formation of transient pores in the cell membrane that permit the passage of linear DNA. Before this, however, the RNAi plasmids were linearized through treatment with I-SceI, a meganuclease that targets telomeric sequences. As two telomeric

sequences exist within the pIBB103 backbone separated by around 800 bp, I-SceI digestion produces a linearized vector and an 800 bp fragment, both of which may be used as positive diagnostics that the digestion worked.

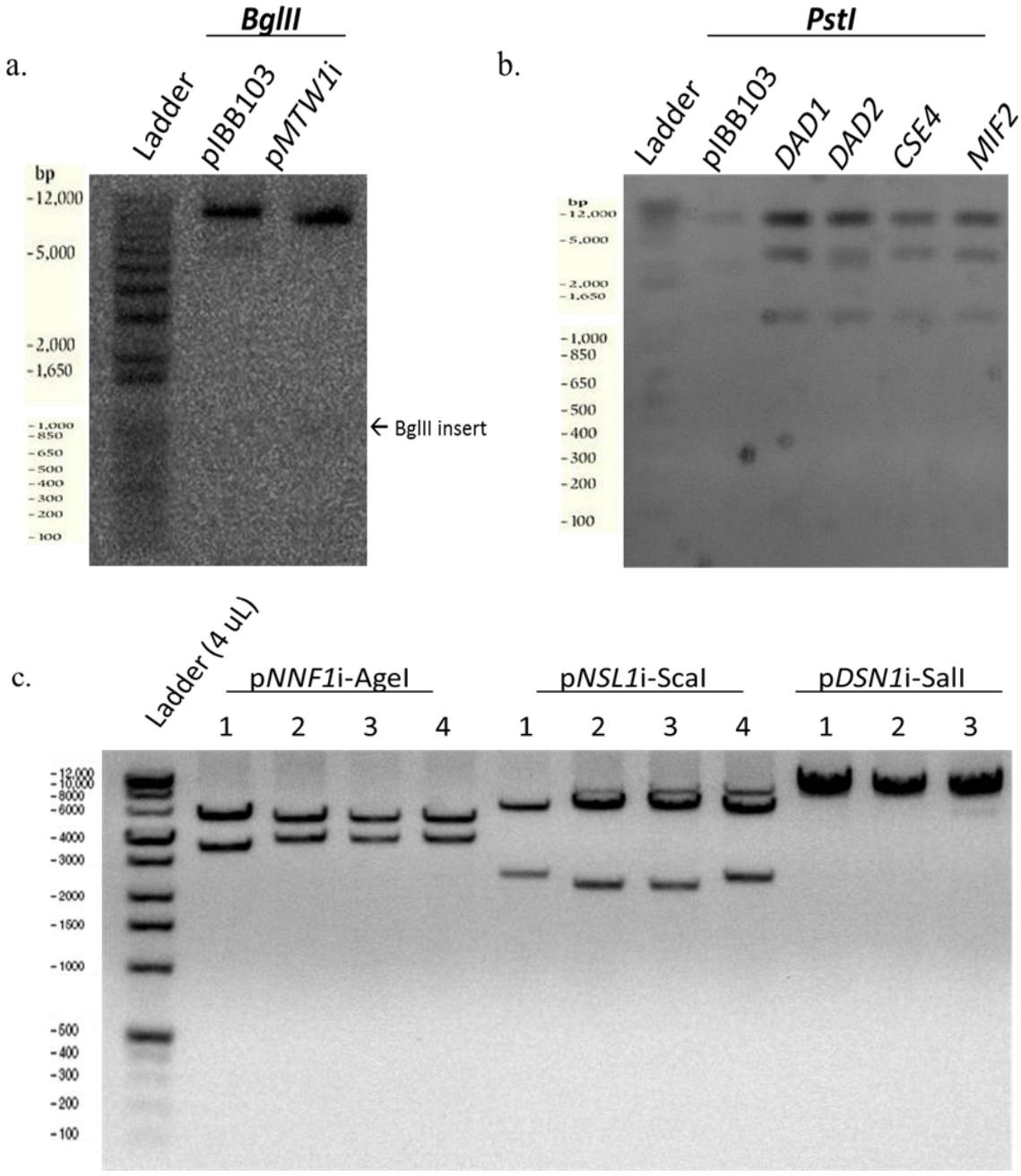

Figure 17. Diagnostic restriction digests of RNAi plasmids. The gels above show the digest products for seven of the kinetochore RNAi plasmids and pIBB103 alone. The first gel (a.) shows PstI digests of pIBB103, p*CSE4*i, p*MIF2*i, p*DAD1*i, and p*DAD2*i. The second gel (b.) shows various digests of p*NNF1*i, p*NSL1*i, and p*DSN1*i.

Plating Results

The results of plating the RNAi transformants are shown below in Figure 18. All of the transformed cells were able to grow on the YPGal/Neo medium as only cells that had taken up the pIBB103 plasmid (with or without an insert) had the neomycin resistance gene. It is likely that the cells were able to grow despite the galactose present on the YPGal/Neo plates because the cells had not yet had enough opportunity to induce the RNAi process. Of the transformants that were plated on the YPGal/Neo plates containing 5-FOA, only those transformed with the p*DAD2*i or p*NSL1*i plasmid were able to grow while those given the p*MTW1*i plasmid grew but at a much slower pace. Cells transformed with vectors containing the *CSE4*, *MIF2*, *NNF1*, *DSN1*, and *DAD2* inserts failed to grow on 5-FOA Gal/Neo. Additionally a negative control consisting of a *Cryptococcus* strain (IBCN #20) containing the neomycin resistance gene integrated into the genome but lacking the RNAi plasmid failed to grow on the 5-FOA Gal/Neo plates. Independent electroporations were performed three times for *MTW1* and two times for the remaining genes.

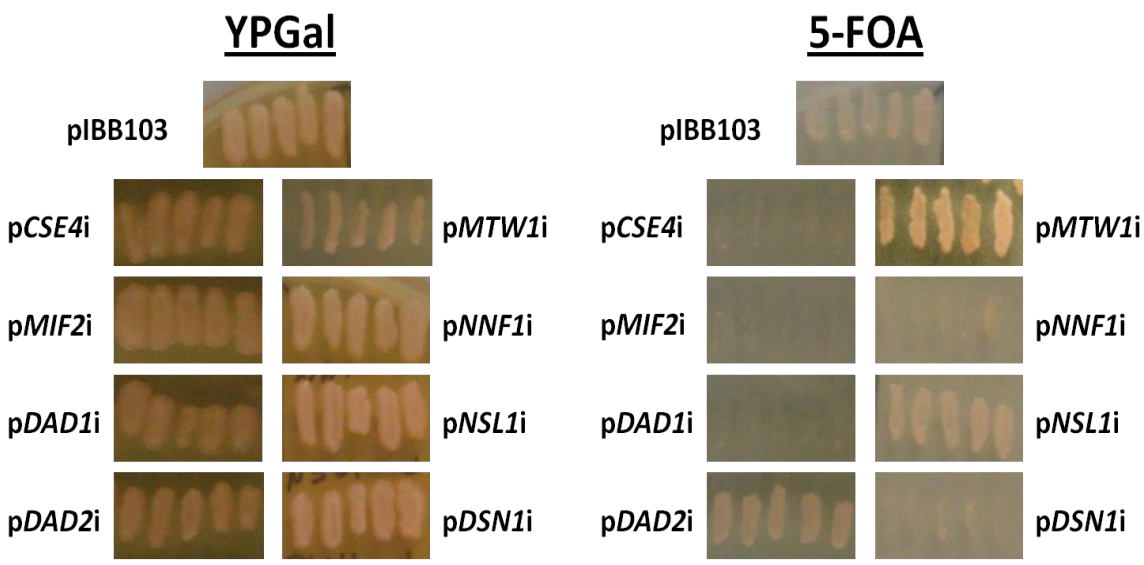

Figure 18. Growth on 5-FOA reveals non-essential roles for some kinetochore genes. The columns on the left show cells that have grown on YPGal/Neo medium while those on the right show cells growing on 5-FOA Gal/Neo.

DISCUSSION AND CONCLUSIONS

Presence of conserved protein sequences in kinetochore homologs

Several putative kinetochore homologs were discovered through amino acid sequence comparison of known kinetochore proteins in previously studied fungal species with the published *C. neoformans* proteome. An analysis of sequence similarities for these putative homologs with known proteins in several ascomycetous species is summarized in Table 4. One conclusion drawn from these comparisons is that the kinetochore proteins of *C. neoformans* are in general more similar to those of *S. pombe* than to those of *S. cerevisiae* or *C. albicans*. Kinetochore proteins show high divergence at the primary sequence level but show conservation in the three-dimensional structure (Petrovic et al., 2010). Homology in kinetochore sequences across fungal species is largely limited to highly conserved domains within each protein (see Supplementary Figures 1 – 6). This phenomenon is perhaps best exemplified by Cse4p, which shows little conservation at the amino terminus but two conserved carboxy-terminal domains with near complete identity between *C. neoformans* and *S. pombe* (Supplementary Figure 1). Cse4p also displays the highest degree of conservation among the proteins examined in these experiments. This is in keeping with expectations as Cse4p is known to make extensive contact with centromeric DNA, leaving little room for evolutionary divergence. CnMif2p (Supplementary Figure 3) also displays two C-terminal conserved domains; these have been widely conserved and interact with other highly conserved protein domains (Meluh and Koshland, 1995). Dad1p and Dad2p (Supplementary Figure 2) are both small proteins that contribute to the outer kinetochore DASH complex. These

proteins show high conservation between *C. neoformans* and other fungi in terms of size and sequence within the amino-terminal region.

Table 4. Global Sequence Comparisons of Kinetochore Homologs.

C. neoformans JEC21	***S. cerevisiae***		***C. albicans***		***S. pombe***	
Putative Homolog	Similarity	Identity	Similarity	Identity	Similarity	Identity
Mtw1p	35.7%	18.6%	25.3%	14.2%	35.8%	17.9%
Cse4p	37.8%	27.3%	48.1%	38.9%	60.3%	51.3%
Mif2p	24.9%	14.5%	28.7%	17.2%	28.7%	18.2%
Dad1p	37.3%	20.3%	33.6%	23.2%	44.1%	24.3%
Dad2p	29.8%	16.8%	38.9%	22.9%	39.6%	25.4%
Nnf1p	16.2%	9.9%	18.5%	8.7%	16.4%	9.5%
Nsl1p	19.3%	8.7%	13.3%	7.4%	12.8%	7.1%
Dsn1p	23.7%	14.5%	28.2%	15.6%	26.3%	15.1%

In terms of the MIND complex, Mtw1p and Dsn1p appear to be more conserved than Nnf1p and Nsl1p. As discussed previously, Mis12p/Mtw1p homologs share two highly conserved domains near the N terminus. These domains may serve as sites of interaction with other conserved kinetochore proteins such as Nnf1p, with which Mtw1p is known to form heterodimers (Hornung et al., 2011). Nsl1p and Mis13p/Dsn1p differ from other kinetochore proteins in that they show regions of high conservation throughout the proteins' sequences (Supplementary Figures 5 and 6, respectively). CnNnf1p (Supplementary Figure 4) shows little overall identity; however, one of the areas most conserved from previously studied species to *C. neoformans* contain residues that constitute an essential coiled-coil domain (Westermann et al., 2003). One intriguing finding is the presence of amino- and carboxy-terminal extensions of varying lengths for each of the *C. neoformans* MIND components. Further investigation revealed that other basidiomycetous species such as *Ustilago maydis* and *Tremella mesenterica* also contain

such extensions in their MIND homologs. These extensions appear to be unique to basidiomycetes as they are not present in previously studied ascomycetous species.

One difference revealed by the amino acid alignment of Mtw1p is the presence of an amino-terminal extension (see Figure 1) in the sequences of the three Basidiomycetous species analyzed (*C. neoformans*, *Ustilago maydis*, and *Tremella mesenterica*). Such a sequence is not seen in the three well studied Ascomycetous species previously mentioned. Amino-terminal and carboxy-terminal extensions are also characteristic of the *Cryptococcus* MIND complex members Nnf1p and Nsl1p. It may be that these terminal extensions play some role in the structure or stability of the final protein. This may be explored by creating partial deletions of these genes, sequentially removing these extensions and studying the effects on cellular growth and morphology. Another intriguing possibility is that these extensions may serve as protein-protein interaction domains that may interact with other proteins in the kinetochore. In order to answer this question, a yeast-two hybrid assay may be performed using only the amino-terminal extension of *CnMtw1* as bait against a *C. neoformans* genomic cDNA library as prey. This would demonstrate potential in vivo interaction with possible binding partners and may help to confirm the role of *CnMtw1* within the kinetochore.

Incubation at elevated temperature leads to enhanced growth inhibition in ts-*mtw1* mutants

The creation of a strain containing a regulatable *MTW1* was thought to be required as this gene is essential for growth and survival in organisms in which it has been previously described (Goshima et al., 1999; Goshima and Yanagida, 2000; Roy and Sanyal, 2011). This gene was therefore predicted to be necessary in *C. neoformans*, thus

preventing the creation of a simple haploid deletion strain. Initial growth assays performed on solid media showed little observable difference between wild type KN99α cells and the two known ts mutant strains. When the ts strains were replica streaked at different temperatures the only distinguishable difference between these strains and the wild type was the diminutive size of the colonies obtained with G109E at 37°C. The results of the spot assays reiterate the finding thus far that *MTW1* is not essential as two mutant strains showed no difference from the wild type in terms of growth. The data obtained from culturing cells in liquid media, however, showed a more distinct and consistent difference in growth rates. The reason growth in liquid media showed more difference between strains may be due to inherent growth potential on solid media that is more limited than that of liquid. In this case, cultures may reach a carrying capacity that is lower on solid media, likely due to the relative lack of space compared to liquid cultures. Such an effect may mask subtle differences in growth rates and explain the differences obtained between solid and liquid media. The doubling time of log phase wild type *C. neoformans* in liquid YPD has been measured at 132 minutes at 24°C, with just over half that time spent in the G_1 phase (Yamaguchi et al., 2007). It is noteworthy that cultures grown on solid media take significantly longer to pass through one cell cycle, having an average doubling time of 200 minutes on average with parent cells doubling twice as quickly as daughter cells. The decreased rate of growth on solid media is hypothesized to be caused by the hypoxic conditions within colonies that do not exist in liquid media (Yamaguchi et al., 2007).

Growth assays in liquid cultures at varying temperatures were performed numerous times. Despite some variability in the relative growth of the two temperature

sensitive mutant strains, a consistent pattern of temperature-sensitivity was observed. In all growth curves performed, after two days growth, both mutant strains had grown equally well as the wild type at permissive temperature but less well than the wild type at the restrictive temperature of 37°C.

Even though such a result implicates Mtw1p as crucial to cell division, this protein does not show the same essentiality to growth as do its homologs in ascomycetous species.

Exaggerated mutant morphologies in response to restrictive conditions

One of the striking observations made during the course of this study was the emergence of highly mutated cell morphologies when mutant cells were grown in restrictive conditions. The ability of *C. neoformans* to survive and grow at 37°C is an established virulence factor (Casadevall and Perfect, 2000) and is crucial for pathogenesis in mammalian hosts. Light microscopy of wild type KN99α cells grown at 37°C revealed the presence of a small percentage of cells with mutant morphology. Such cells appear to have attempted to reproduce and bud but were unable to do so correctly. These cells may for example have an elongated daughter bud that is not coccal in shape and can be up to several times larger than the parent cell. Mutant cells in a wild type population like this represent a background rate of cell-cycle dysfunction at the restrictive temperature.

As shown by the bud counting data and the DIC micrographs, mutant phenotypes were both more extreme and significantly more common in the both the ts mutant strains and the P_{CTR4}-*MTW1* strain as compared to the wild type. Individual cells were present with numerous budding protrusions emanating from a central parent cell. Other cells were seen in which a bud would sprout on the opposite side as an earlier bud that had mostly formed but failed to complete cytokinesis. Yet other mutant cells had

morphologies composed of several extended cells joined together at the ends to form chains. Mutant phenotypes such as these are strongly indicative of cytokinetic defects that prevent normal cell division. The inability of budding cells to perform cytokinesis is often associated with gross errors in chromosome segregation due to nondisjunction, spindle checkpoint malfunction, and kinetochore failure. It is therefore reasonable to assume that the mutant phenotypes observed are caused by such a breakdown of kinetochore function, resulting in the cytokinetic failures responsible for multiple-budded mutant phenotypes. Indeed, previous studies have yielded similar phenotypes when studying mutations in genes known to be critical to cell-cycle function. A recent study reported similar elongated "pseudohyphal-like" budding morphologies when studying temperature sensitive mutants of *MTW1* in *C. albicans*. Similar results were also obtained in that study from ts-*cacse4* mutants (Roy and Sanyal, 2011). The first two studies performed on *MTW1* orthologs also revealed similar budding anomalies with many cells stuck in the G_2/M transition as large-budded cells (Goshima et al, 1999; Goshima and Yanagida, 2000). The fact that the budding state distributions for the temperature-sensitive cells grown at 37°C are strikingly similar to that obtained for the P_{CTR4}-*MTW1* strain lends credence to the idea that *CnMTW1* plays a central role in kinetochore function.

RNA interference reveals essential functions for several kinetochore homologs

The vector into which the amplified kinetochore sequences were inserted is pIBB103, a plasmid designed to initiate the RNAi process in cryptococcal cells. As shown in Figure 19 below, pIBB103 contains a neomycin resistance gene under a cryptococcal promoter along with two telomeric sequences spaced about 800 bp apart.

The RNAi cassette within pIBB103 contains two *GAL7* promoters flanking a segment of the *URA5* gene. This region also contains restriction sites that allow insertion of the gene of interest between the *GAL7* promoter regions alongside the *URA5* fragment. Terminator sequences are present outside this region on both sides that stop transcription being driven by the *GAL7* promoter on the opposite side of the cassette.

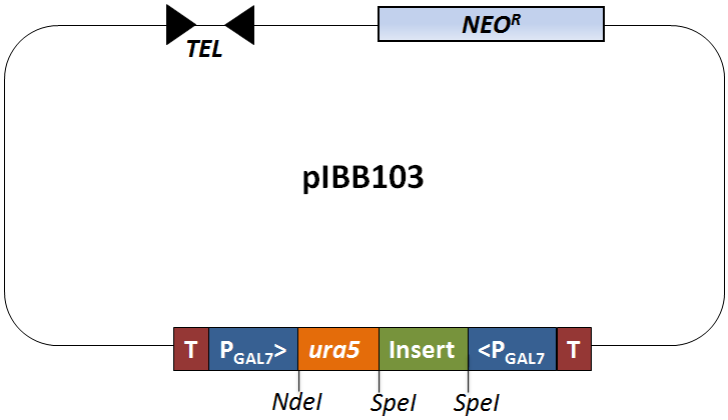

Figure 19. RNAi Vector pIBB103. P_{GAL7} represents the GAL7 promoter while T represents the transcription terminator for the promoter on the opposite side of the insert region. Black triangles denote telomeric sequences.

The *URA5* gene fragment acts as a selective marker for cells that are performing RNAi efficiently (Bose and Doering, 2011). The *URA5* gene codes for an enzyme that converts 5-fluoroorotic acid into 5-fluorouracil. This product may then be incorporated into mRNA and prevent further polymerization due to the fluorine group replacing the 5' hydroxyl group essential to the chemistry of polymerization. By including the *URA5* fragment in between the *GAL7* promoters one can select for cells that are actively performing RNAi by plating them on 5 FOA galactose-containing medium. Cells that are performing RNAi and that have been transformed with the pIBB103 plasmid will survive on 5-FOA medium as the transcription of the URA5 gene product is silenced and the conversion of 5-FOA to 5-fluorouracil will not occur. Cells transformed with the

pIBB103 vector containing a fragment of the gene of interest may or may not grow on 5-FOA medium depending on whether the gene is non-essential or essential, respectively. If cells transformed with a plasmid containing a gene of interest fail to grow on 5-FOA while those receiving only the pIBB103 plasmid without an added gene succeed in growing it is implicative that the gene of interest is essential for viability in this species.

Results from the several rounds of plating of the RNAi plasmid-transformed cells suggest that *CSE4*, *MIF2*, *NNF1*, *DSN1*, and *DAD1* may be essential while *DAD2*, *NSL1*, and *MTW1* appear to be nonessential. *MTW1*, though likely nonessential, may still be important for proper cell growth. This is thought to be the case due to the relatively slow growth observed in MTW1 transformed cells as compared to the pIBB control. This effect has been observed both on 5-FOA Gal/Neo plates and in YPGal/Neo liquid media. This result for *MTW1* is consistent with those obtained from the temperature-sensitive mutants which indicate a non-essential but nonetheless important role for *MTW1* in cell division.

The results obtained for the other MIND complex members are similar to those obtained in previous studies that indicate essentiality for Nnf1p, Nsl1p, and Dsn1p in *S. cerevisiae* with one exception (Westermann et al., 2003; Euskirchen, 2002). p*NSL1*i-transformed cells grew on 5-FOA media, indicating a non-essential role for this putative homolog in contrast with that of the *S. cerevisiae* protein. This difference may be due to some difference in kinetochore structure between members of these fungal clades. Another, however, is the misidentification of the *NSL1* gene in *C. neoformans*. As these other MIND complex members had not been studied before in *C. neoformans*, identification of these putative homologs was based solely on protein sequence homology

with the most recently published version of the *C. neoformans* proteome. The DELTA-BLAST search for this Nsl1p homolog yielded only a few results with low homology. In addition, Nsl1p showed only 16% identity among a few selected fungal species in a previous study (Meraldi et al., 2006). For these reasons it is possible that the correct locus was not isolated for *CnNSL1* and further work will need to be done on this locus and other putative loci. Attempts to delete members of the MIND complex have all resulted in inviability (Shan 1997, Euskirchen 2002). RNAi repression of MIND complex members in human cells results in chromosome segregation errors and impaired recruitment of outer kinetochore proteins to the centromere (Kline et al., 2006). Despite the fact that deletions of *CSE4* homologs are invariably lethal, some species may tolerate up to 90% reduction in expression (Verdaasdonk and Bloom, 2011). Such findings may possibly explain why the strain transformed with p*NSL1*i grew: RNAi is a knockdown technique that is not uniformly efficient in *C. neoformans* (Bose and Doering, 2011). This may also explain why one of the ten p*NNF1*i transformant colonies selected grew on 5-FOA media, while the other nine failed to grow (data not shown).

The Cryptococcal genes *CSE4*, *MIF2*, and *DAD1* all yielded lethal phenotypes when silenced by this RNAi screen, implying that these are essential for viability. These results agree with those obtained from mutational analysis in other fungal species (Meluh and Koshland, 2003; Stoler et al., 1995; Miranda et al., 2005). This RNAi screen also found *CnDAD2* to be non-essential for cell cycle progression. This conflicts with previous studies on the DASH complex and may possibly be due to differences in the molecular workings of basidiomycetous yeasts. Another member of the DASH complex may be compensating for the loss of *DAD1* function; further experiments may be

performed to screen for synthetic lethal mutants to assess potential relationships between members of this complex in *C. neoformans*.

The next path of investigation will involve performing total RNA extractions from RNAi plasmid transformed cells that are grown in either YPGal Neo liquid media or 5-FOA Gal-Neo liquid media. Once the RNA is collected from the cells it will be used as template to generate cDNAs representing only those genes being expressed at the time of collection. PCRs can be performed using these cDNAs as template in an attempt to see if the genes targeted for RNAi-induced silencing are in fact turned off. Analyzing the results of these PCRs by gel electrophoresis will show whether mRNA from the targeted genes is present or not. If the mRNA is not present (i.e. no PCR product can be made from the cDNA template) then we can infer that the gene has been silenced and that the growth patterns of transformed cells are a result of decreased or absent kinetochore mRNAs.

Another course of investigation is to create and study deletion strains of the genes that were shown to be non-essential. Creation of a deletion strain involves using a series of primers designed to replace the gene being studied with an antibiotic resistance gene as a selective marker. If the gene is indeed non-essential then the cells carrying this deletion should still survive. These cells will then be subject to study so that the function of the missing gene may be inferred. One such way to study this in the *Cryptococcal* kinetochore would be to microscopically observe the localization of various other kinetochore proteins along with the cell nucleus. If in the absence of the gene of interest the other kinetochore proteins are mis-localized or if the overall cell morphology is

aberrant then it may be inferred that these non-essential proteins still play some role in kinetochore function and cell division.

Summary

Cryptococcus neoformans is an opportunistic pathogen that may potentially be lethal in immunocompromised individuals and kills more than 624,000 people per year, a group largely comprised of HIV-positive individuals in sub-Saharan Africa where there is little access to medicine (Park et al., 2009). As this species is resistant to most modern antibiotics due to its associated virulence factors a need exists for more potent therapies with fewer side effects. In addition, such resistant species of yeasts often exhibit aneuploidy, the improper segregation of chromosomes during cell division. The molecular biology concerning cellular reproduction and division in *C. neoformans* is poorly understood among fungal pathogens. Most research on such fungi has focused on ascomycetous species such as *Saccharomyces cerevisiae* and as such it is unknown whether basidiomycotes such as *C. neoformans* perform crucial cellular processes in the same way. The results generated from this study provide a foundation for further research into the functioning of the cryptococcal kinetochore. We have demonstrated that *MTW1* likely serves largely the same role as its orthologs do for their species, with the exception that *CnMTW1* is not essential for viability. We have also demonstrated essential roles for a number of kinetochore genes. Additionally, non-essential roles have been shown for three kinetochore genes; this is in direct contrast to other species in which orthologous genes are essential. This finding may provide a basis for further study of these genes through gene deletion. The cryptococcal MIND complex was specifically

addressed during the course of this study; no previous work has been published on these genes in *C. neoformans* and thus this work represents a first attempt to describe these genes and their functions. Identification of these three genes is still putative; further work must be done to positively confirm their identity as MIND complex orthologs. Understanding how chromosome segregation occurs in *C. neoformans* may bring about better therapies: if it can be shown that homologous proteins perform the same actions in *Cryptococcus* then these proteins may become the focus for understanding how these fungal cells induce aneuploidy in response to antifungal drugs.

REFERENCES

Benham RW. 1950. Cryptococcosis and Blastomycosis. Annals of the New York Academy of Sciences. 50: 1299 – 1314.

Boratyn GM, AA Schäffer, R Agarwala, SF Altschul, DJ Lipman, TL Madden. 2012. Domain enhanced lookup time accelerated BLAST. Biology Direct. 7: 12.

Bose I, T Doering. 2011. Efficient implementation of RNA interference in the pathogenic yeast *Cryptococcus neoformans*. Journal of Microbiological Methods. 86: 156 – 159.

Casadevall A, JR Perfect. 1998. Cryptococcus neoformans. American Society for Microbiology. Washington, D.C.

Chan GK, ST Liu, TJ Yen. 2005. Kinetochore structure and function. Trends in Cell Biology. 15(11): 589 – 598.

Cheeseman IM, C Brew, M Wolyniak, A Desai, S Anderson, N Muster, JR Yates, TC Huffaker, DG Drubin, G Barnes. 2001. Implication of a novel multiprotein Dam1p complex in outer kinetochore function. The Journal of Cell Biology. 155(7): 1137 – 1145.

Cox GM, J Mukherjee, GT Cole, A Casadevall, JR Perfect. 2000. Urease as a virulence factor in experimental cryptococcosis. Infection and Immunity. 68: 443–448.

Cox GM, HC McDade, SC Chen, SC Tucker, M Gottfredsson, LC Wright, TC Sorrell, SD Leidich, A Casadevall, MA Ghannoum, JR Perfect. 2001. Extracellular phospholipase activity is a virulence factor for *Cryptococcus neoformans*. Molecular Microbiology. 39: 166–175.

Davidson RC, JR Blankenship, PR Kraus, M de Jesus-Berrios, CM Hull, C D'Souza, P Wang, J Heitman. 2002. A PCR-based strategy to generate integrative targeting alleles with large regions of homology. Microbiology. 148: 2607 – 2615.

de Wulf P, AD McAinsh, PK Sorger. 2003. Hierarchical assembly of the budding yeast kinetochore from multiple subcomplexes. Genes & Development. 17: 2902 – 2921.

Dumesic PA, P Natarajan, C Chen, IA Drinnenberg, BJ Schiller, J Thompson, JJ Moresco, JR Yates III, DP Bartel, HD Madhani. 2013. Stalled spliceosomes are a signal for RNAi-mediated genome defense. Cell. 152(5): 957 – 968.

Enache-Angoulvant A, J Chandenier, F Symoens, P Lacube, J Bolognini, C Douchet, JL Poirot, C Hennequin. 2007. Molecular identification of *Cryptococcus neoformans* serotypes. Journal of Clinical Microbiology. 45(4): 1261 – 1265.

Euskirchen GM. 2002. Nnf1p, Dsn1p, Mtw1p, and Nsl1p: a new group of proteins important for chromosome segregation in *Saccharomyces cerevisiae*. Eukaryotic Cell. 1(2): 229 – 240.

Goshima G, S Saitoh, M Yanagida. 1999. Proper metaphase spindle length is determined by centromere proteins Mis12 and Mis6 required for faithful chromosome segregation. Genes & Development. 13: 1664 – 1677.

Goshima G, M Yanagida. 2000. Establishing biorientation occurs with precocious separation of the sister kinetochores, but not the arms, in the early spindle of budding yeast. Cell. 100: 619 – 633.

Goshima G, O Iwasaki, C Obuse, M Yanagida. 2003. The role of PpeI/PP6 phosphatase for equal chromosome segregation in fission yeast kinetochore. The EMBO

Journal. 22: 2752 – 2763.

Gouet P, E Courcelle, DI Stuart, M Métoz. 1999. ESPript: analysis of multiple sequence alignments in PostScript. Bioinformatics. 15(4): 305 – 308.

Hornung P, M Maier, GM Alushin, GC Lander, E Nogales, S Westermann. 2011. Molecular architecture and connectivity of the budding yeast Mtw1 kinetochore complex. Journal of Molecular Biology. 405: 548 – 559.

Kline SL, IM Cheeseman, T Hori, T Fukagawa, A Desai. 2006. The human Mis12 complex is required for kinetochore assembly and proper chromosome segregation. The Journal of Cell Biology. 173(1): 9 – 17.

Kraus PR, MJ Boily, SS Giles, JE Stajich, A Allen, GM Cox, FS Dietrich, JR Perfect, J Heitman. 2004. Identification of *Cryptococcus neoformans* temperature-regulated genes with a genomic-DNA microarray. Eukaryotic Cell. 3(5): 1249 – 1260.

Kwon-Chung KJ, JC Rhodes. 1986. Encapsulation and melanin formation as indicators of virulence in *Cryptococcus neoformans*. Infection and Immunity. 51**:** 218–223.

Loftus BJ, E Fung, P Roncaglia, D Rowley, P Amedeo, D Bruno, J Vamathevan, M Miranda, IJ Anderson, JA Fraser, JE Allen, IE Bosdet, MR Brent, R Chiu, TL Doering, MJ Donlin, CA D'Souza, DS Fox, V Grinberg, J Fu, M Fukushima, BJ Haas, JC Huang, G Janbon, SJM Jones, HL Koo, MI Krzywinski, JK Kwon-Chung, KB Lengeler, R Maiti, MA Marra, RE Marra, CA Mathewson, TG Mitchell, M Pertea, FR Riggs, SL Salzburg, JE Schein, A Shvartsbeyn, H Shin, M Shumway, CA Specht, BB Suh, A Tenney, TR Utterback, BL Wickes, JR Wortman, NH Wye, JW Kronstad, JK Lodge, Joseph Heitman, RW Davis, CM Fraser, RW Hyman. 2005. The Genome of the basidiomycetous yeast and human

pathogen *Cryptococcus neoformans*. Science. 307: 1321 – 1324.

Maskell DP, XW Hu, MR Singleton. 2010. Molecular architecture and assembly of the yeast kinetochore MIND complex. The Journal of Cell Biology. 190(5): 823 – 834.

Medoff G, GS Kobayashi, CN Kwan, D Schlessinger, P Venkov. 1972. Potentiation of rifampicin and 5-fluorocytosine as antifungal antibiotics by amphotericin B. Proceedings of the National Academy of Sciences USA. 69(1): 196 – 199.

Meeks-Wagner D, JS Wood, B Garvik, LH Hartwell. 1986. Isolation of two genes that affect mitotic chromosome transmission in S. cerevisiae. Cell. 44(1): 53 – 63.

Meluh PB, D Koshland. 1995. Evidence that the *MIF2* gene of *Saccharomyces cerevisiae* encodes a centromere protein with homology to the mammalian centromere protein CENP-C. Molecular Biology of the Cell. 6: 793 – 807.

Meluh PB, P Yang, L Glowczewski, D Koshland, MM Smith. 1998. Cse4p is a component of the core centromere of *Saccharomyces cerevisiae*. Cell. 94: 607 – 613.

Meraldi P, AD McAinsh, E Rheinbay, PK Sorger. 2006. Phylogenetic and structural analysis of centromeric DNA and kinetochore proteins. Genome Biology. 7(3): R23.1 – R23.21.

Miranda JJL, P De Wulf, PK Sorger, SC Harrison. 2005. The yeast DASH complex forms closed rings on microtubules. Nature Structural & Molecular Biology. 12(2): 138 – 143.

Nekrasov VS, MA Smith, S Peak-Chew, JV Kilmartin. 2003. Interactions between centromere complexes in *Saccharomyces cerevisiae*. Molecular Biology of the

Cell. 14: 4931 – 4946.

Ory JJ, CL Griffith, TL Doering. 2004. An efficiently regulated promoter system for *Cryptococcus neoformans* utilizing the *CTR4* promoter. Yeast. 21: 919 – 926.

Papadopoulos JS, R Agarwala. 2007. COBALT: constraint-based alignment tool for multiple protein sequences. Bioinformatics. 23(9): 1073 – 1079.

Park BJ, KA Wannemuehler, BJ Marston, N Govender, PG Pappas, TM Chiller. 2009. Estimation of the current global burden of cryptococcal meningitis among persons living with HIV/AIDS. AIDS. 23(4): 525 – 530.

Petrovic A, S Pasqualato, P Dube, V Krenn, S Santaguida, D Cittaro, S Monzani, L Massimiliano, J Keller, A Tarricone, A Maiolica, H Stark, A Musacchio. 2010. The MIS12 complex is a protein interaction hub for outer kinetochore assembly. The Journal of Cell Biology. 190(5): 835 – 852.

Roy B, K Sanyal. 2011. Diversity in requirement of genetic and epigenetic factors for centromere function in fungi. Eukaryotic Cell. 10(11): 1384 – 1395.

Roy B, LS Burrack, MA Lone, J Berman, K Sanyal. 2011. CaMtw1, a member of the evolutionarily conserved Mis12 kinetochore protein family, is required for efficient inner kinetochore assembly in the pathogenic yeast *Candida albicans*. Molecular Microbiology. 80(1): 14 – 32.

Rice P, I Longden, A Bleasby. 2000. *EMBOSS: The European Molecular Biology Open Software Suite*. Trends in Genetics. 16(6): 276 – 277.

Sanyal K, M Baum, J Carbon. 2004. Centromeric DNA Sequences in the pathogenic yeast *Candida albicans* are all different and unique. Proceedings of the National Academy of Sciences. 101(31): 11374 – 11379.

Semighini CP, AF Averette, JR Perfect, J Heitman. 2011. Deletion of Cryptococcus neoformans AIF ortholog promotes chromosome aneuploidy and Fluconazole-resistance in a metacaspase-independent manner. PLoS Pathogens. 7(11): 1 – 21.

Shan X, Z Xue, G Euskirchen, T Mélèse. 1997. *NNF1* is an essential yeast gene required for proper spindle orientation, nucleolar and nuclear envelope structure and mRNA export. Journal of Cell Science. 110: 1615 – 1624.

Sia RA, KB Lengeler, J Heitman. 2000. Diploid strains of the pathogenic basidiomycete *Cryptococcus neoformans* are thermally dimorphic. Fungal Genetics and Biology. 29: 153 – 163.

Sionov E, H Lee, YC Chang, KJ Kwon-Chung. 2010. *Cryptococcus neoformans* overcomes stress of azole drugs by formation of disomy in specific multiple Chromosomes. PLoS Pathogens. 6(4): 1 – 13.

Stoler S, KC Keith, KE Curnick, M Fitzgerald-Hayes. 1995. A mutation in *CSE4*, an essential gene encoding a novel chromatin-associated protein in yeast, causes chromosome nondisjunction and cell cycle arrest at mitosis. Genes & Development. 9: 573 – 586.

Toffaletti DL, TH Rude, SA Johnston, DT Durack, JR Perfect. 1993. Gene transfer in *Cryptococcus neoformans* by use of biolistic delivery of DNA. Journal of Bacteriology. 175(5): 1405.

Verdaasdonk JS, K Bloom. 2011. Centromeres: unique chromatin structures that drive chromosome segregation. Nature Reviews Molecular Cell Biology. 12: 320 – 332.

Wei RR, J Al-Bassam, SC Harrison. 2007. The Ndc80/HEC1 complex is a contact point for kinetochore-microtubule attachment. Nature Structural & Molecular Biology.

14: 54 – 59.

Westermann S, IM Cheeseman, S Anderson, JR Yates III, DG Drubin, G Barnes. 2003. Architecture of the budding yeast kinetochore reveals a conserved molecular core. The Journal of Cell Biology. 163(2): 215 – 222.

Yamaguchi M, M Ohkuso, SK Biswas, S Kawamoto. 2007. Cytological study of cell cycle of the pathogenic yeast *Cryptococcus neoformans*. Japanese Journal of Medical Mycology. 48: 145 – 152.

APPENDIX

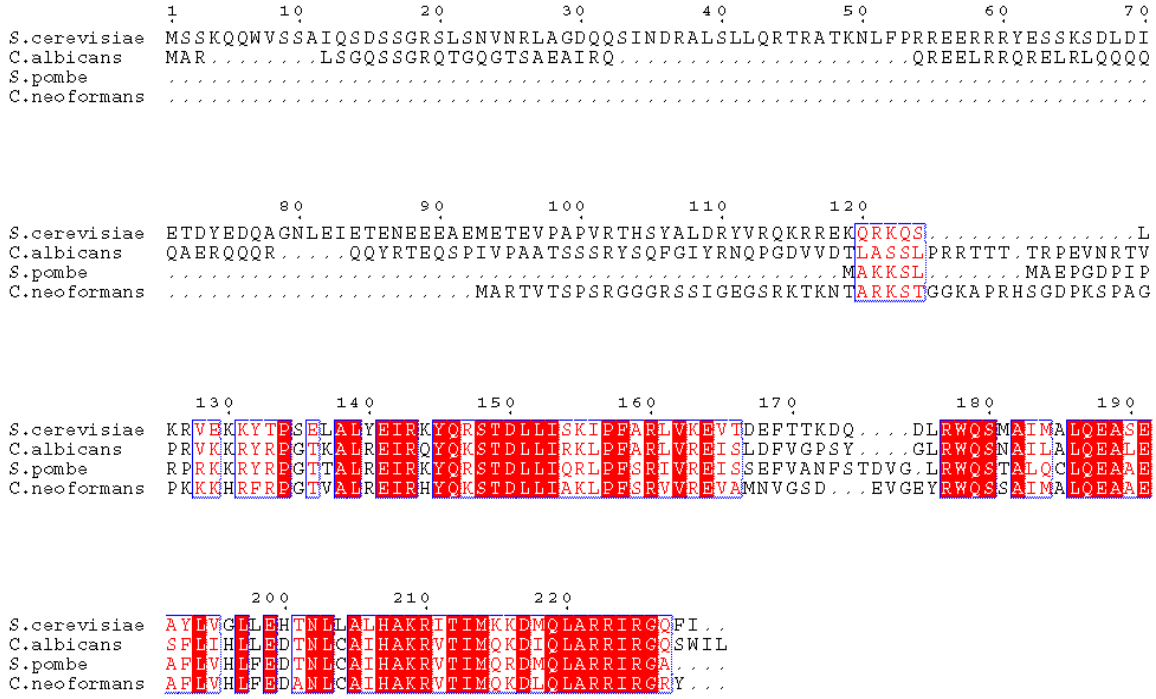

A1. Cse4p Sequence Alignment

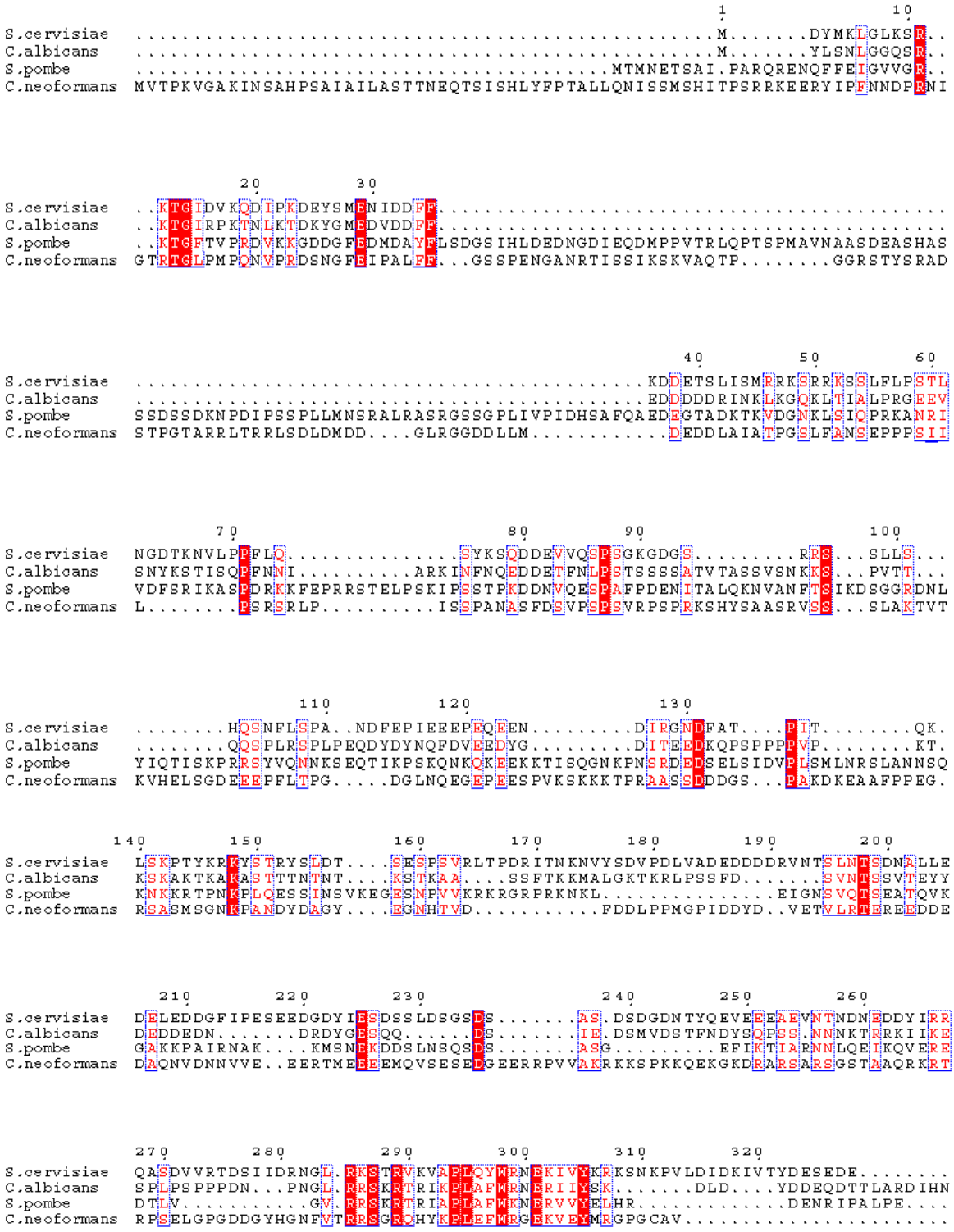

A2. Mif2p Sequence Alignment.

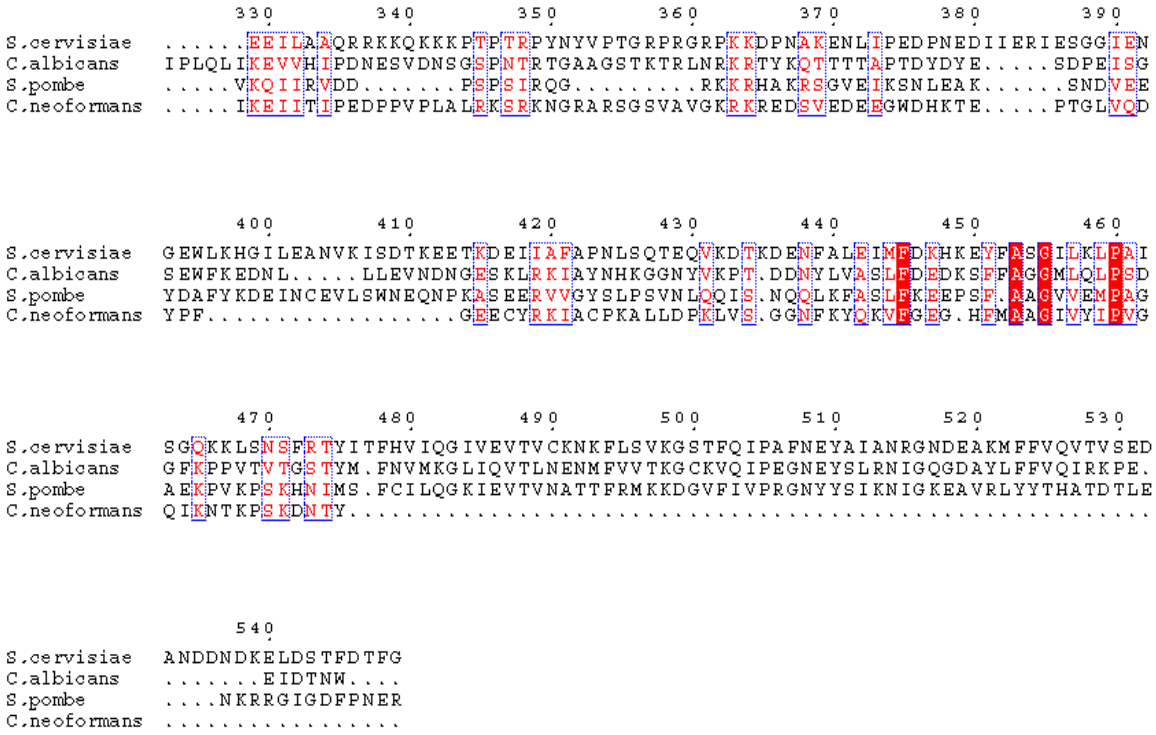

A2. Mif2p Sequence Alignment Continued.

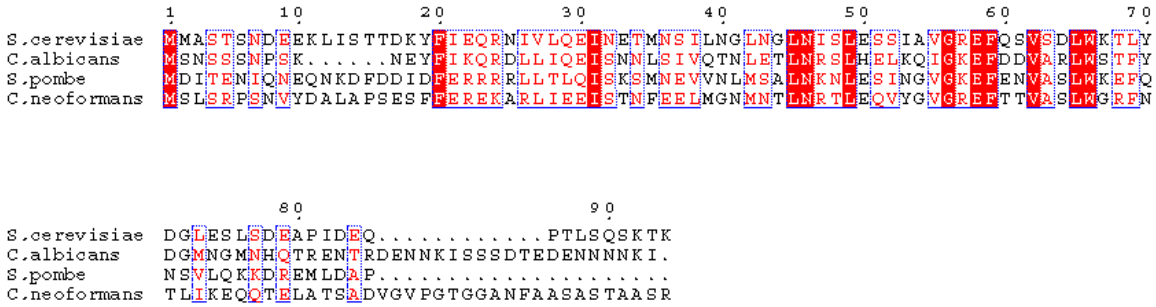

A3. Dad1p Sequence Alignment.

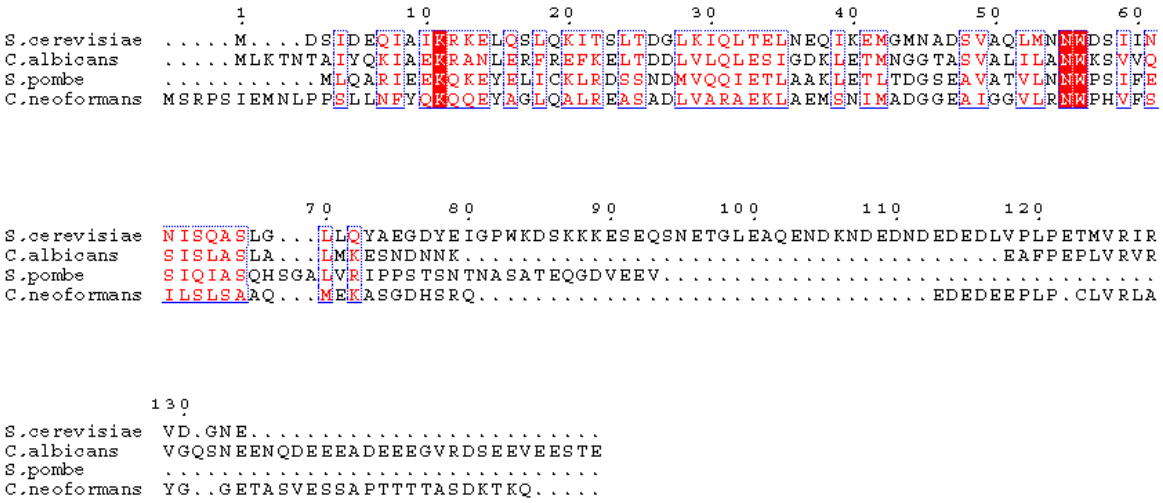

A4. Dad2p Sequence Alignment.

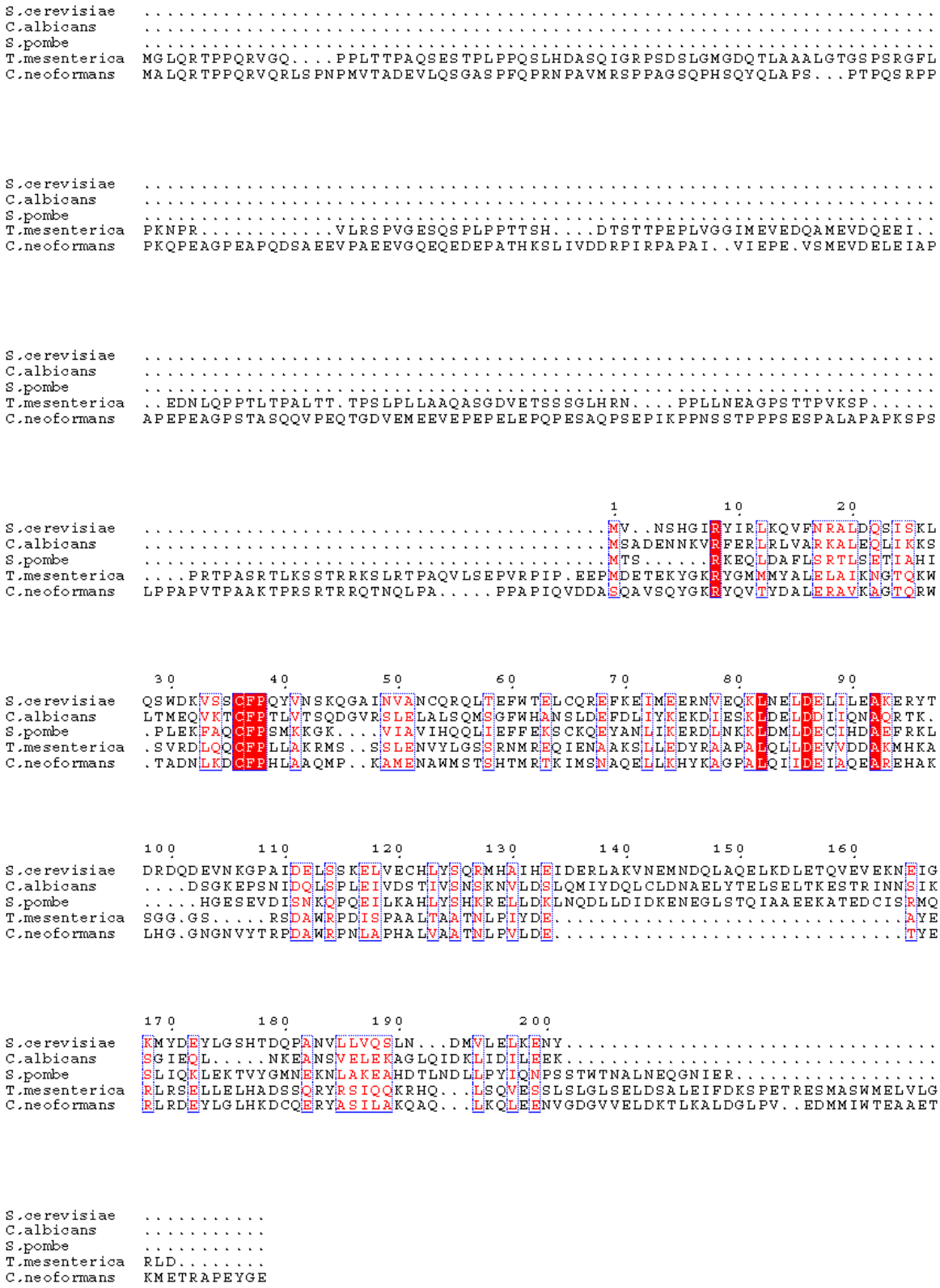

A5. Nnf1p Sequence Alignment.

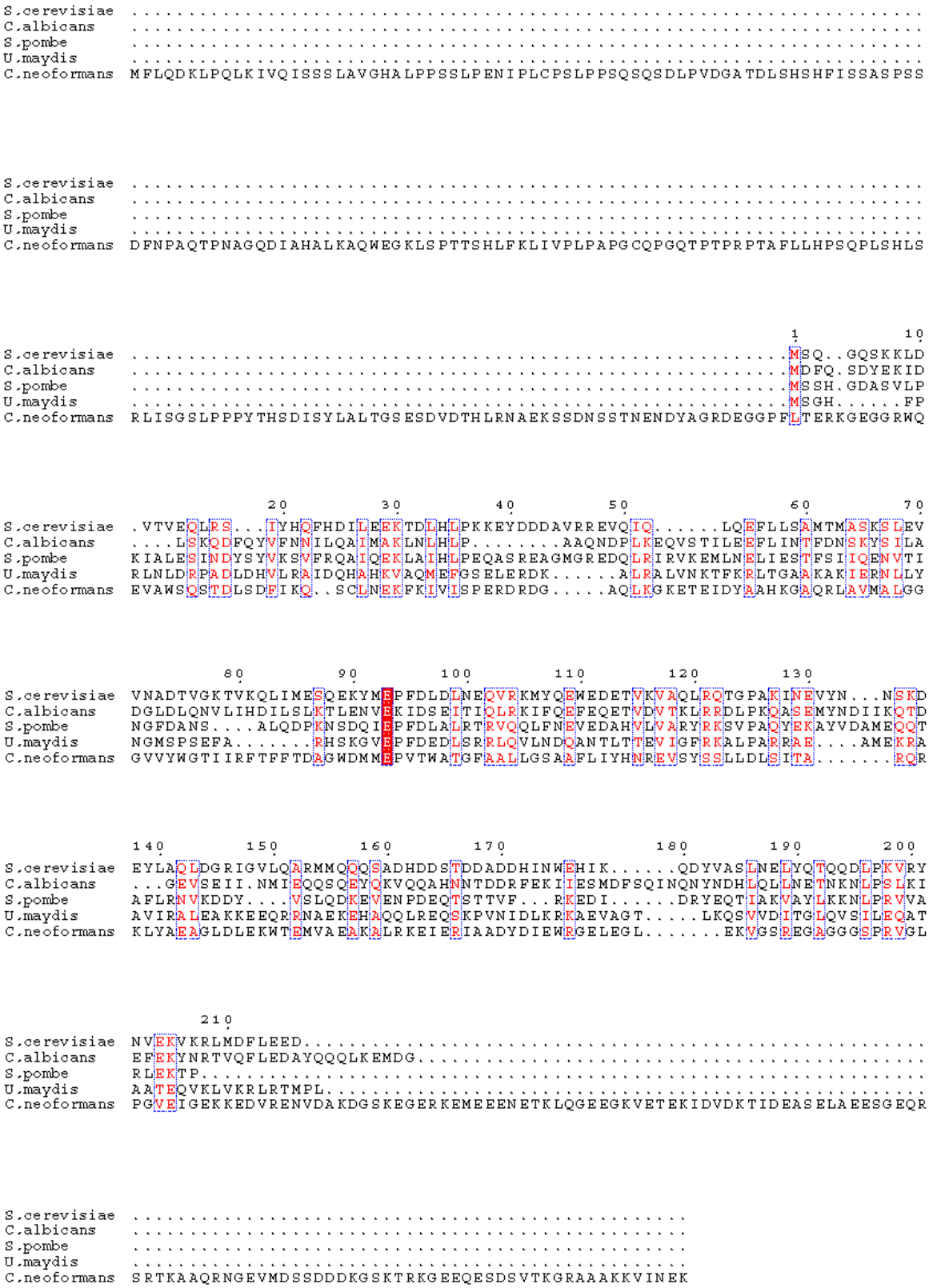

A6. Nsl1p Sequence Alignments.

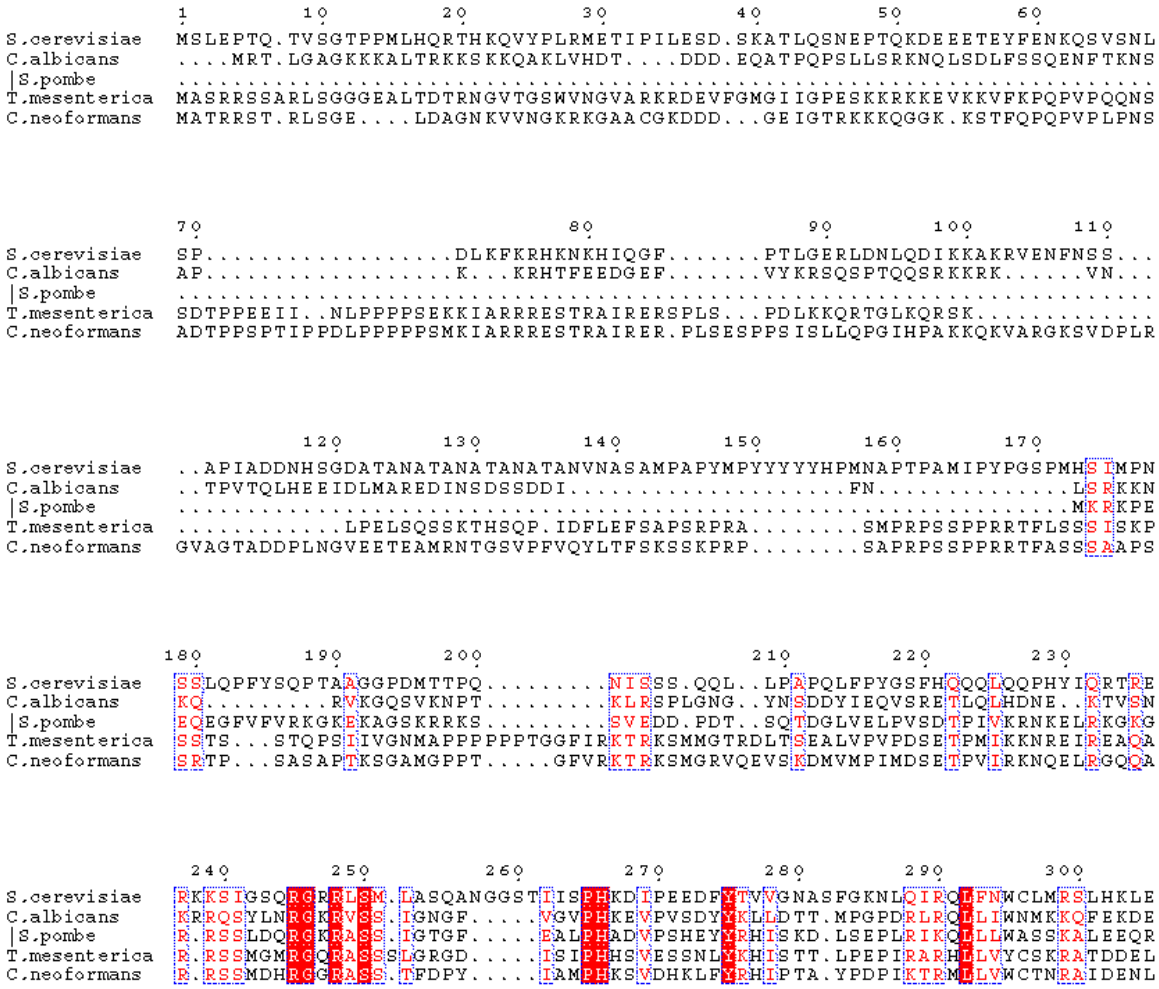

A7. Dsn1p Sequence Alignment.

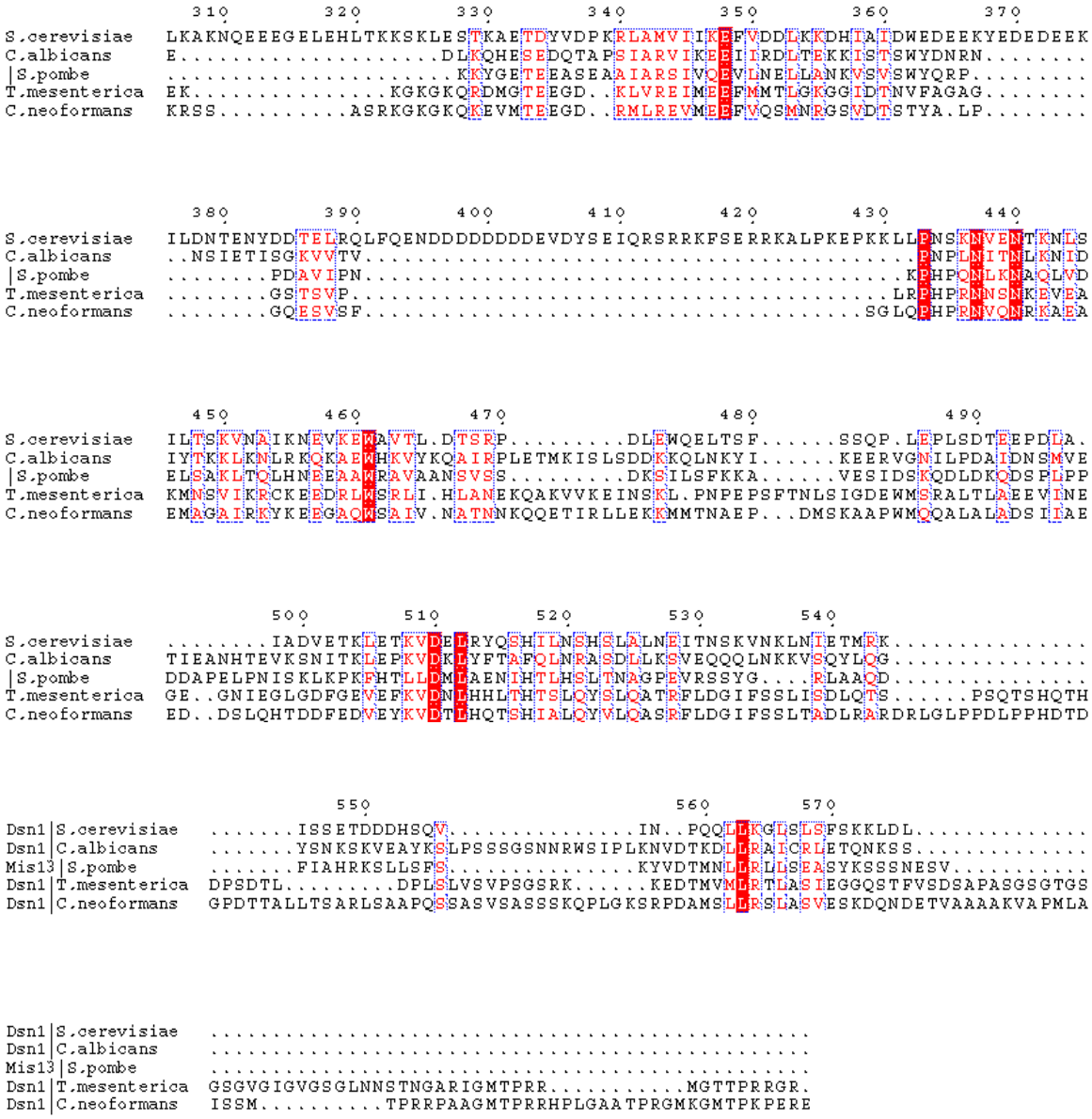

A7. Dsn1p Sequence Alignment Continued.